Applied Energy 328 (2022) 120117

Contents lists available at ScienceDirect

Applied Energy

journal homepage: www.elsevier.com/locate/apenergy

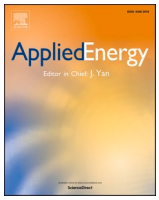

Optimal resilient allocation of mobile energy storages considering coordinated microgrids biddings

Ainollah Rahimi Sadegh [a], Mehrdad Setayesh Nazar [a], Miadreza Shafie-khah [b], João P.S. Catalão [c]

[a] Shahid Beheshti University, Tehran, Iran
[b] School of Technology and Innovations, University of Vaasa, 65200 Vaasa, Finland
[c] Faculty of Engineering of the University of Porto and INESC TEC, 4200-465 Porto, Portugal

HIGHLIGHTS

- An integrated framework for MESSs allocation in the active distributions system is presented.
- The integrated model regulating reserve transactions between ADS and microgrids is presented.
- The proposed solution methodology compromises two-stage optimization processes.
- The proposed algorithm successfully increased the self-healing index by about 49.88%.

ARTICLE INFO

Keywords:
Active distribution network
Mobile energy storage facilities
Microgrids
Coordinated bidding
Electricity market

ABSTRACT

This paper presents an algorithm for optimal resilient allocation of Mobile Energy Storage Systems (MESSs) for an active distribution system considering the microgrids coordinated bidding process. The main contribution of this paper is that the impacts of coordinated biddings of microgrids on the allocation of MESSs in the day-ahead and real-time markets are investigated. The proposed optimization framework is another contribution of this paper that decomposes the optimization process into multiple procedures for the day-ahead and real-time optimization horizons. The active distribution system can transact active power, reactive power, spinning reserve, and regulating reserve with the microgrids in the day-ahead horizon. Further, the distribution system can transact active power, reactive power, and ramp services with microgrids on the real-time horizon. The self-healing index and coordinated gain index are introduced to assess the resiliency level and coordination gain of microgrids, respectively. The proposed algorithm was simulated for the 123-bus test system. The method reduced the average value of aggregated operating and interruption costs of the system by about 60.16% considering the coordinated bidding of microgrids for the worst-case external shock. The proposed algorithm successfully increased the self-healing index by about 49.88% for the test system.

1. Introduction

Mobile Energy Storage Systems (MESSs) are utilized to increase the resiliency of electrical distribution systems in external shock conditions. The Active Distribution System Operator (ADSO) should utilize preventive/corrective measures to mitigate the impacts of external shocks considering the contributions of Distributed Energy Resources (DERs). The MESSs can be optimally allocated in the system's zones in a preventive way. Further, the ADSO can dispatch the MESSs and other DERs in a corrective manner to recover the system after tolerating the external shocks. The DERs may compromise Distributed Generation (DG) facilities, Plug-in Hybrid Electric Vehicle (PHEV) Parking Lots (PLs), Smart Homes (SHs), Wind Turbines (WTs), PhotoVoltaic (PV) arrays, Combined Heat and Power (CHP) units, and Electrical energy Storage Systems (ESSs) [1].

Over the recent years, different aspects of resilient operational scheduling of active distribution systems have been presented considering the commitment scenarios of MESSs. As shown in Table 1, the optimal resilient scheduling of distribution system can be categorized into the following groups: 1) the optimal scheduling of system resources considering commitment scenarios of stationary ESSs and MESSs, and 2) the optimal scheduling of system resources without commitment scenarios of MESSs.

E-mail address: catalao@fe.up.pt (J.P.S. Catalão).

https://doi.org/10.1016/j.apenergy.2022.120117
Received 17 June 2022; Received in revised form 17 September 2022; Accepted 5 October 2022
Available online 30 October 2022

Nomenclature

Abbreviation

ADS	Active Distribution System
ADSO	Active Distribution System Operator
AMG	Active MicroGrids
ARIMA	Autoregressive Integrated Moving Average
CHP	Combined Heat and Power
CIC	Customer Interruption Cost
CGI	Coordination Gain index
DA	Day-Ahead
DER	Distributed Energy Resource
DG	Distributed Generation
ESS	Electrical energy Storage System
HEMS	Home Energy Management System
MESS	Mobile Energy Storage System
PL	Parking Lot
PHEV	Plug-in Hybrid Electrical Vehicle
PV	Photovoltaic
RT	Real-Time
SHs	Smart Homes
SHI	Self-Healing Index
WT	Wind Turbine

Parameters

c_{AMG}^{RT}	The AMG electricity generation cost in the real-time market
$c_{AMG}^{RAMP^+}$	The AMG ramp-up cost in the real-time market
$c_{AMG}^{RAMP^-}$	The AMG ramp-down cost in the real-time market
$F_{ADS\_LINE}^{Max}$	The maximum flow limit of ADS feeder
W, W',W"	Weighting factors

Sets

EXSS	Set of the probable external shock scenarios
DERNS	The set of the normal operating scenarios of the ADSO DERs.
NL	The set of the system loads
Ξ	The set of the operating states scenarios of AMGs

Variables

C_{MESS}	The aggregated operational and transportation costs of MESS
P^{ADS}	Active power of distribution system
P^{CHP}	Active power of CHP
P^{SH}	Active power of smart home
P^{WT}	Active power of wind turbine
P^{PV}	Active power of photovoltaic array
P^{PL}	Active power of parking lot
P^{CL}	Active power of critical load
P^{NCL}	Active power of non-critical load
D	Duration of deferrable non-critical load commitment
P^{DG}	Active power of distributed generation facility
P^{ESS}	Active power of energy storage
P^{MESS}	Active power of MESS
$P^{AMGTRANS}$	Transaction with AMGs
$P^{ADSLoss}$	Active power loss
$P^{WMTRANS}$	Transaction with wholesale market
$\lambda_{AMG}^{SR\_DA}$	The submitted value of the AMG day-ahead spinning reserve price
$\lambda_{AMG}^{AP\_DA}$	The submitted value of the AMG day-ahead active power price
$\lambda_{AMG}^{RP\_DA}$	The submitted value of the AMG day-ahead reactive power price
$\lambda_{AMG}^{RR\_DA}$	The submitted value of the AMG day-ahead regulation reserve price
SR_{AMG}^{DA}	The day-ahead accepted values of AMG spinning reserve
P_{AMG}^{DA}	The day-ahead accepted values of AMG active power
Q_{AMG}^{DA}	The day-ahead accepted values of AMG reactive power
RR_{AMG}^{DA}	The day-ahead accepted values of AMG regulating reserve
C_{AMG}^{DA}	The day-ahead operating cost of AMG
$\lambda_{AMG}^{AP\_RT}$	The submitted values of AMG real-time market active power price
$\lambda_{AMG}^{AP\_RT}$,$\lambda_{AMG}^{RAMP^+}$,$\lambda_{AMG}^{RAMP^-}$	The submitted values of AMG real-time market ramp-up price
$\lambda_{AMG}^{AP\_RT}$,$\lambda_{AMG}^{RAMP^+}$,$\lambda_{AMG}^{RAMP^-}$	The submitted values of AMG real-time market ramp-down price
P_{AMG}^{RT}	The accepted value of AMG active power in the real-time market
$P_{AMG}^{RAMP^+}$	The accepted values of AMG ramp-up active power in the real-time market
$P_{AMG}^{RAMP^-}$	The accepted values of AMG ramp-down active power in the real-time market
$\lambda_{ADSO}^{AP\_DA}$	The submitted value of the ADSO day-ahead active power price
$\lambda_{ADSO}^{RP\_DA}$	The submitted value of ADSO day-ahead reactive power price
$\lambda_{ADSO}^{AP\_RT}$	The submitted values of the ADSO real-time market active power price
$\lambda_{ADSO}^{RP\_RT}$	are the submitted values of the ADSO real-time market reactive power price
P_{ADSO}^{DA}	The day-ahead accepted value of ADSO active power
Q_{ADSO}^{DA}	The day-ahead accepted value of ADSO reactive power
P_{ADSO}^{RT}	The accepted value of the ADSO real-time market active power
Q_{ADSO}^{RT}	The accepted value of the ADSO real-time market reactive power
P_{ADS_LINE}	Active power of ADS feeder
Q_{ADS_LINE}	Reactive power of ADS feeder
V	Voltage of ADS bus
X	Binary decision variable of boundary line
Y	Non-critical load supply decision variable
Z	Binary decision variable for allocating of MESSs in the available locations

Based on the above categorization and for the first group, Ref. [2] proposed a three-level defender–attacker–defender model to allocate MESSs in a preventive way. The upper-level problem determined the optimal dispatch of energy resources for a certain contingency. The second and third level problems optimized the total load shedding of microgrids and the final dispatch of energy resources of DERs, respectively. Ref. [3] introduced a model that considered MESSs in the system's optimal power flow. The objective function minimized the operating costs of the system and MESSs' operating costs. The coordinated biddings of microgrids and smart homes' commitment in the MESSs allocation problem were not simulated in Refs. [2,3]. Further, the real-time operation of the system in the presence of MESSs was not modeled.

Ref. [4] proposed a four-phase optimization model to allocate MESSs. The first and second phases compromised data collection and MESSs selection, respectively. The third and fourth phases modeled the

Table 1
Comparison of the proposed method with other papers.

References		1	2	3	4	5	6	7	8	9	10	11	12	13	14	15	16	17	18	19	20	21	22	23	24	25	Proposed Approach
Coordinated bidding of MGs		×	×	×	×	×	×	×	×	×	×	×	×	×	×	×	×	×	×	×	×	×	×	×	×	×	✓
Switching of system in ext. shock		×	×	×	×	×	×	×	×	×	×	×	×	×	×	×	×	✓	×	✓	×	✓	✓	×	✓	×	✓
Commitment of smart homes		×	×	×	×	×	×	×	×	×	×	×	×	×	×	×	×	×	×	×	×	×	×	×	×	×	✓
Real-time pricing		×	×	×	×	×	×	×	×	×	×	✓	×	✓	×	×	×	×	×	×	×	×	×	×	×	✓	✓
Ancillary Services of PLs		×	×	×	×	×	×	×	×	×	×	×	×	×	×	×	×	×	×	×	×	×	×	×	×	×	✓
Coordination Gain index		×	×	×	×	×	×	×	×	×	×	×	×	×	×	×	×	×	×	×	×	×	×	×	×	×	✓
Ramp Market		×	×	×	×	×	×	×	×	×	×	×	×	×	×	×	×	×	×	×	×	×	×	×	×	✓	✓
Method	MILP	✓	×	✓	✓	×	×	✓	✓	✓	×	×	×	✓	✓	×	✓	✓	×	×	×	×	×	×	×	×	×
	MINLP	×	×	×	×	×	✓	×	×	×	×	×	×	×	×	×	×	×	×	×	×	✓	×	✓	×	×	×
	Heuristic	×	✓	×		✓	×	×	×	×	✓	✓	✓	×	×	✓	×	×	✓	✓	✓	×	✓	×	✓	✓	✓
Model	Determ.	×	×	✓	✓	✓	✓	✓	✓	×	✓	✓	✓	×	×	✓	×	✓	✓	✓	✓	×	✓	✓	✓	×	×
	Stoch.	✓	✓	×	×	×	×	×	×	✓	×	×	×	✓	✓	×	✓	×	×	×	×	✓	×	×	×	✓	✓
Objective Function	ADSO Benefit	✓	×	×	×	×	×	×	×	×	×	×	×	✓	✓	✓	×	×	×	×	×	×	×	×	×	✓	✓
	Gen. Cost	✓	✓	✓	✓	✓	✓	✓	✓	✓	✓	✓	×	✓	✓	✓	✓	✓	✓	✓	✓	✓	✓	×	✓	✓	✓
	SHs Benefit	×	×	×	×	×	×	×	✓	×	×	×	×	×	×	×	×	×	×	×	×	×	×	×	×	×	×	✓
	PLs Benefit	×	×	×	×	×	×	×	×	×	×	×	×	×	×	×	×	×	×	×	×	×	×	×	×	✓	✓
	Storage Cost	✓	×	✓	✓	✓	✓	✓	✓	×	✓	✓	×	✓	✓	✓	✓	×	×	×	×	×	×	×	✓	✓	✓
	Secu. Costs	✓	✓	✓	✓	✓	✓	✓	✓	✓	×	×	×	✓	✓	×	×	×	✓	×	✓	✓	✓	✓	×	✓	✓
	PHEV cost	✓	×	×	×	×	×	×	×	×	✓	×	✓	✓	✓	×	✓	×	×	×	×	×	×	×	×	✓	✓
	WT	✓	✓	×	×	×	×	×	×	×	✓	×	×	×	✓	×	✓	×	×	×	×	×	×	×	×	✓	✓
	PV	✓	✓	×	×	×	×	×	×	×	✓	✓	×	×	✓	×	×	×	×	×	×	×	×	×	×	✓	✓
DA-Market		✓	✓	✓	✓	✓	✓	✓	✓	✓	✓	✓	✓	✓	✓	✓	✓	✓	✓	✓	×	✓	×	×	✓	✓	✓
RT- Market scheduling		✓	×	×	×	×	×	×	×	×	×	×	×	×	✓	×	×	×	×	×	×	×	×	×	×	✓	✓

PHEVs' impacts on the optimization process and optimal location of MESSs, respectively. Ref. [5] introduced a two-stage optimization process to reduce voltage unbalance using MESSs. The optimization process considered the DERs fluctuations uncertainties. The model quantified the uncertainties of DERs on the voltage unbalance. The real-time operational conditions, bidding strategies of active microgrids, and system switching in shock conditions were not assessed in Refs. [4,5].

Ref. [6] assessed a model to maintain the electricity supply of critical loads in emergency conditions. The MESSs and distributed generation facilities were utilized to supply loads. A mixed integer quadratic programming method optimization process was used to solve the problem. Ref. [7] evaluated a two-step optimization algorithm to determine the optimal size, location, and operating scheduling of stationary and mobile energy storage facilities. The first and second steps determined the allocation of energy storage facilities and operating problems, respectively. Refs. [6,7] did not consider the real-time operation, smart homes model, and microgrids contribution scenarios in the MESSs optimal allocation problem.

Ref. [8] explored the resiliency of distribution system considering MESSs and distributed generation facilities. The heating loads, DERs, and demand response programs were considered in the model. The linearization technique was adopted to solve the problem. Ref. [9] proposed a two-stage robust optimization process to consider the uncertainties of outages and determine the optimal dispatching patterns of MESSs in critical conditions. The real-time operation, microgrids' strategies, and system sectionalizing process were not modeled in Refs. [8,9].

Based on the above categorization and for the second group, Ref. [10] assessed a model that considered the interactions between distribution system operator, DGs' owners, parking lots, and

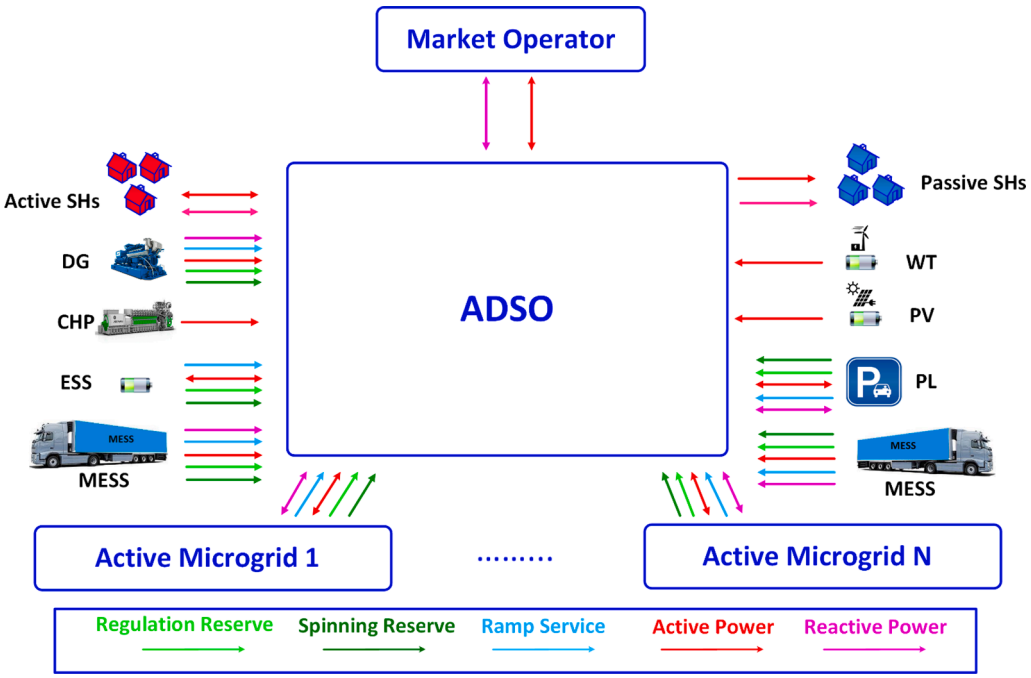

Fig. 1. The interaction between different entities of the system.

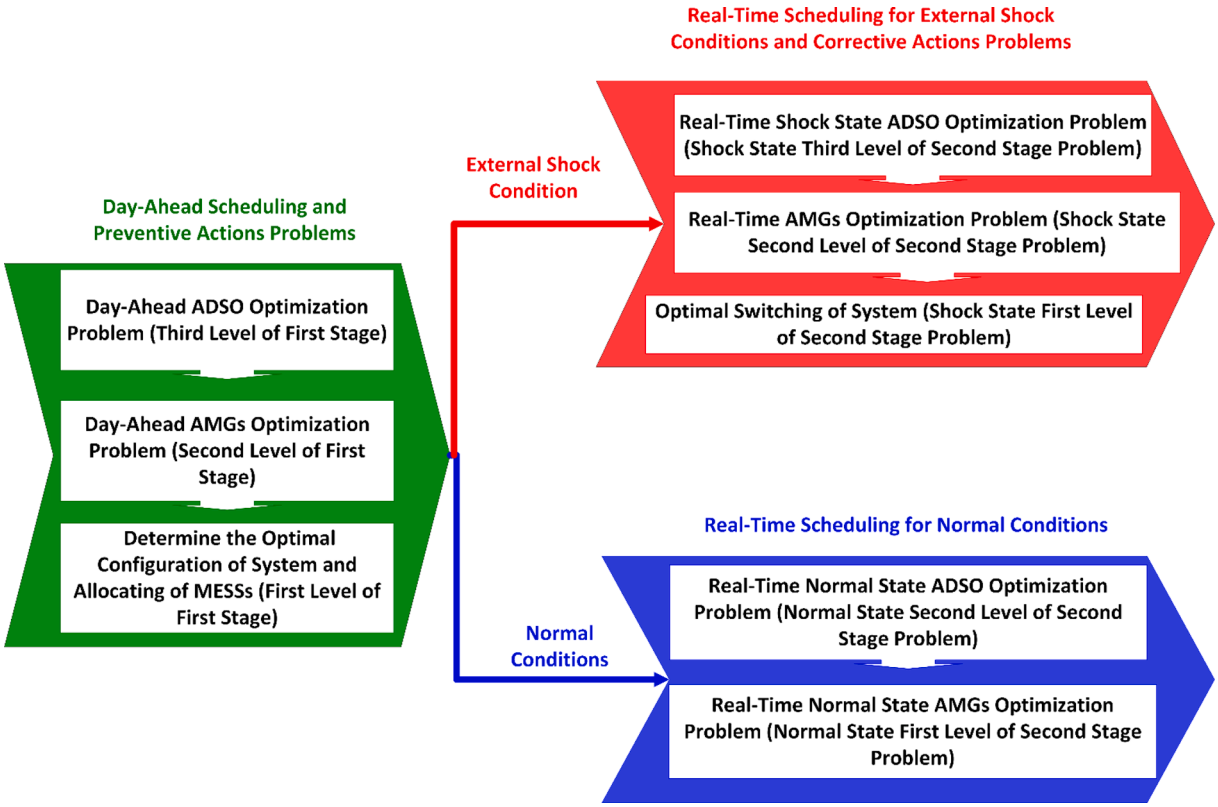

Fig. 2. The procedure of the proposed optimization algorithm.

intermittent electricity generations. The fuzzy decision-making process was utilized to find the optimal values of the multi-objective model. Ref. [11] explored the plug-in electric vehicle commitment impacts on the system scheduling. The uncertainties of loads, microgrids commitments, electricity generations, and prices were modeled. Ref. [12] proposed an optimization algorithm to enhance the resiliency system considering DERs commitment scenarios and household appliances' characteristics. The results revealed that the electric vehicle contributions highly enhanced the resiliency of the system. The impacts of the sectionalizing process, real-time market, and microgrid biddings on the MESSs allocating problem were not explored in Refs. [10-12].

Ref. [1] evaluated an optimization algorithm to enhance the

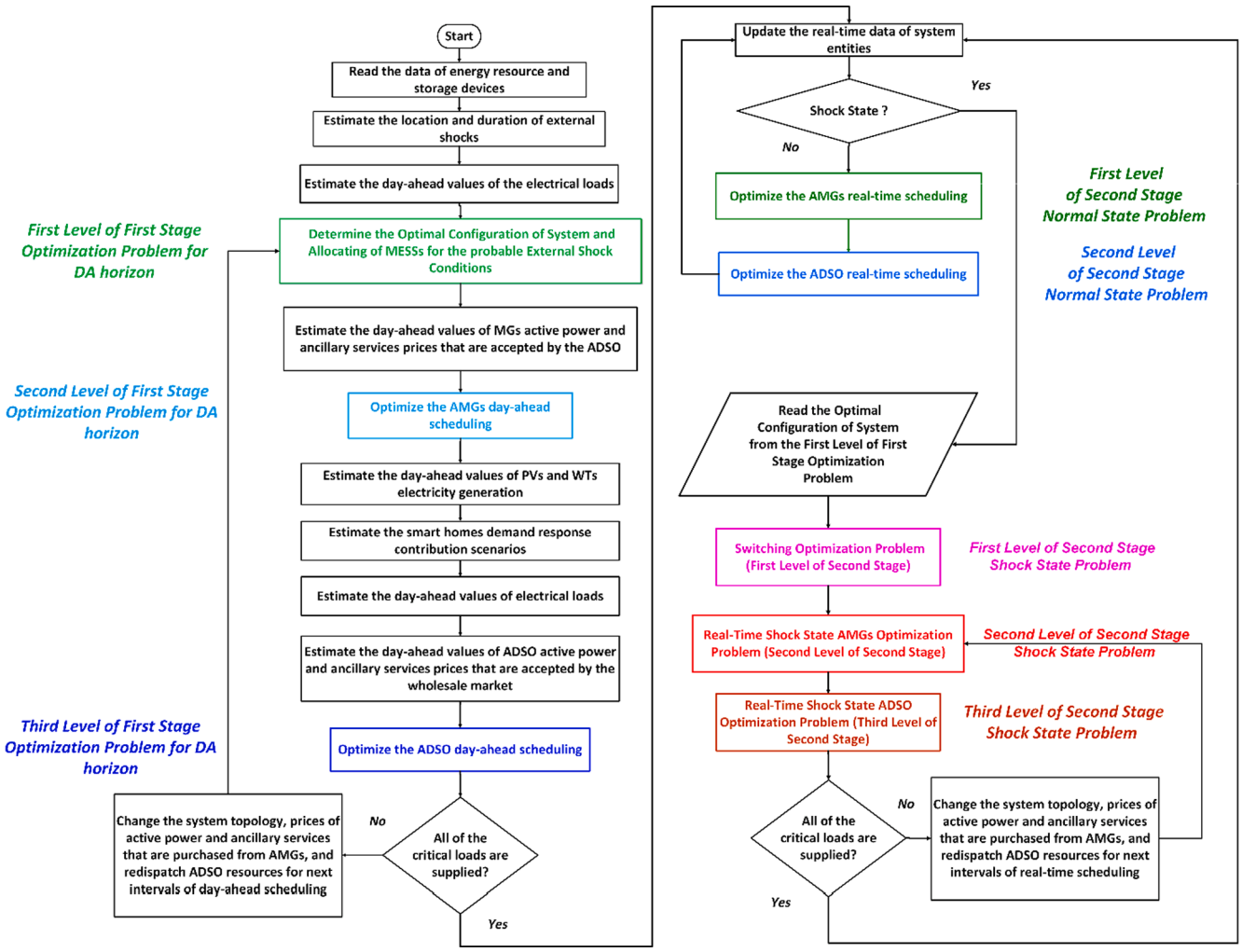

Fig. 3. The day-ahead and real-time optimization processes.

resiliency of the system considering the capacity withholding of DERs. The proposed model decreased the expected costs of the 123-bus IEEE test system by about 88% concerning the case without the proposed method. The coordinated biddings of microgrids, smart homes' commitment, MESSs allocation process, and the ramp market were not modeled in Ref. [1]. Ref. [13] assessed an optimization process to enhance the resiliency of the system considering electric vehicles and demand response programs. The stochastic programming utilized a conditional value at risk model to determine the risk-averse values of system costs. Ref. [14] proposed a resilient enhancement algorithm that compromised a two-stage optimization process considering the customers' comfort level. The optimization process compromised day-ahead and real-time energy management of microgrids and determined the optimal energy transactions of distributed energy resources. Refs. [13,14] did not encounter the smart homes' commitment biddings of microgrids in their models in the MESSs allocation.

Ref. [15] introduced an emergency demand response process to enhance the resiliency of a system, reduce costs, and the aging of system facilities. The aging of facilities and reliability of the system were considered. Ref. [16] evaluated an optimization algorithm to maximize the resiliency of an electrical system. The uncertainties of intermittent electricity generation facilities, electric vehicles, and demand response programs were considered. The optimization results showed that the proposed method reduced the system costs by about 84%. The bidding strategies of microgrids and real-time market were not considered in Refs. [15,16]. Ref. [17] proposed a model to schedule the DERs of networked microgrids considering the sectionalizing process to mitigate the impacts of external shocks. The optimization process utilized demand response programs to minimize operating costs. Ref. [17] did not assess the impacts of bidding strategies of microgrids on the MESSs allocation. Ref. [18] proposed a three stages model to enhance the resiliency of the system. The hardening and switching processes were carried out in the first and second stages, respectively. The service restoration was performed in the third stage. Ref. [13] utilized two-stage stochastic chance-constrained programming to increase the resiliency of the system. The adjustable and interruptible loads were considered in the optimization process. The smart homes' commitment and microgrids' biddings in MESSs optimal allocation were not assessed in Refs. [13,18].

Ref. [19] proposed a sectionalizing process for a distribution system that clustered the system into multi-microgrids in contingent conditions. The optimization process utilized a fuzzy satisfying model to reduce the values of voltage deviations, energy loss, energy not supplied, and reactive power not supplied. Ref. [20] sectionalized the distribution system into microgrids to enhance the resiliency of the system. The mixed integer non-linear programming model minimized the operating costs. The impacts of microgrids' biddings and smart homes on the MESSs allocation were not modeled in Ref [19,20]. Further, the real-time market simulation was not carried out in Refs. [19,20].

Ref. [21] assessed a model to enhance the resiliency of networked microgrids. The analytical hierarchical algorithm was implemented to determine the optimal values of the composite resiliency index.

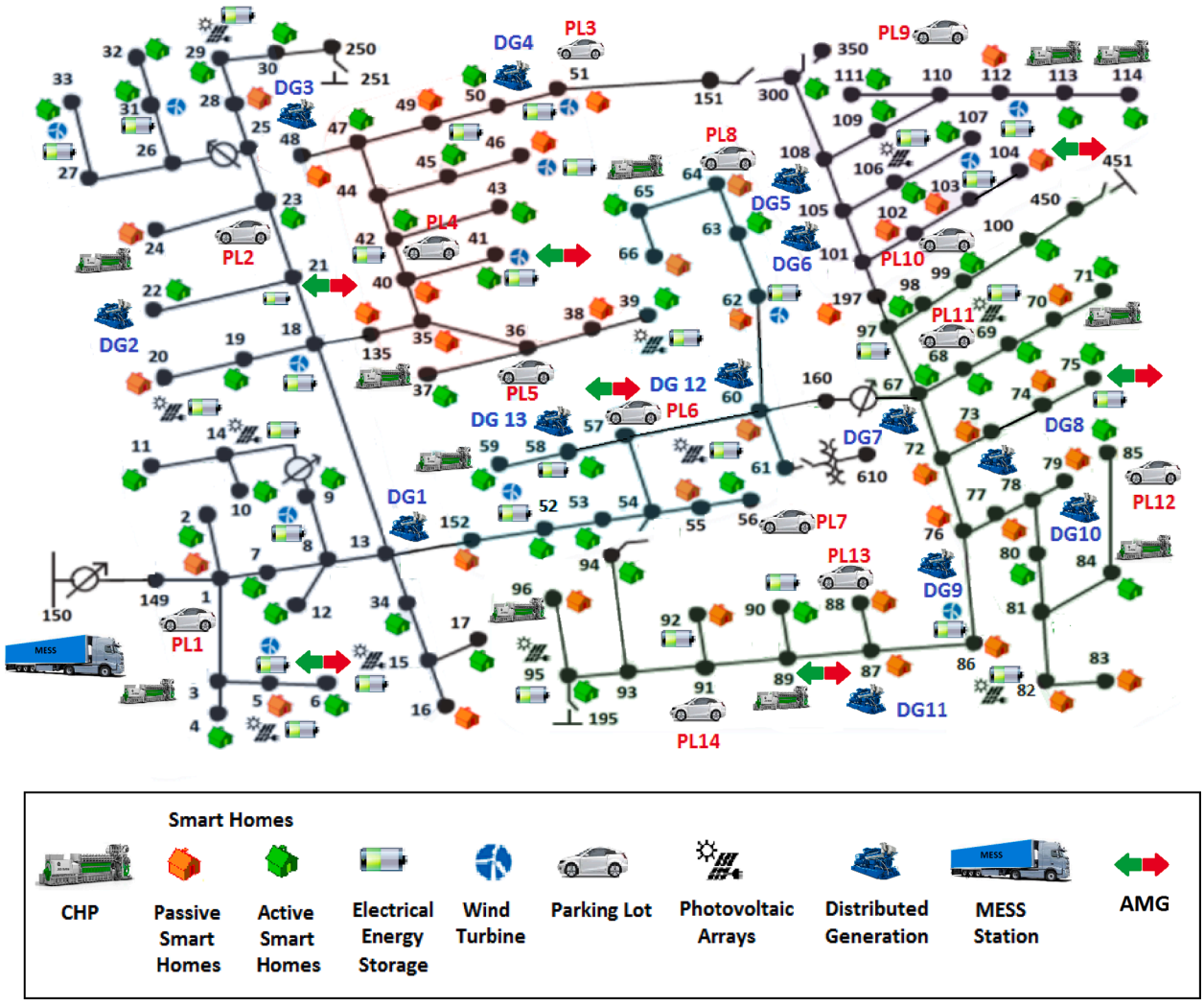

Fig. 4. The 123-bus IEEE test system.

Ref. [22] carried out a simulation process to find the optimal microgrid formation of the distribution system. The model maximized the restored loads using iterative linear programming. The bidding strategies of microgrids, smart homes contributions, and real-time operational conditions were not explored in Refs. [21,22]. Ref. [23] utilized a model to schedule the distribution system and microgrids in the first and second stages, respectively. The first and second stages optimized the scheduling of microgrids and the restoration process of the distribution system, respectively. Two hierarchical and centralized optimization algorithms were considered. Ref. [24] proposed a multi-stage optimization approach to enhance the resiliency of multi-carrier energy systems. The proposed model considered the preventive/corrective actions for day-ahead and real-time markets. The coordinated biddings of microgrids, sectionalizing process, ramp market, and smart homes' commitment were not considered in Refs. [23,24].

Based on the above descriptions of recent papers and as shown in Table 1, the main contributions of this paper can be summarized as follows:

- An integrated framework for MESSs allocation in the active distributions system considering ramp market, sectionalizing of the system, coordinated biddings of microgrids, and smart homes' commitment, is presented.
- The integrated model of active power, reactive power, spinning reserve, and regulating reserve transactions between Active Distribution System (ADS) and microgrids in the day-ahead market is presented. Power transactions between ADS and microgrids in the real-time market are also considered.
- The proposed solution methodology compromises two-stage optimization processes for day-ahead and real-time optimization horizons. The self-healing index is proposed to assess the impacts of MESSs allocations on distribution system resiliency. Also, the coordination gain index evaluates the impacts of coordinated biddings of microgrids.

2. Problem Modeling and Formulation

Fig. 1 presents the interactions between the electricity market, ADSO, intermittent electricity generation facilities, distributed generation units, smart homes, electrical energy storage systems, parking lots, and PHEVs.

As shown in Fig. 1, active power, reactive power, spinning reserve, and regulating reserve are transacted in the day-ahead market by the ADS, Active MicroGrids (AMGs), and wholesale market. Further, the active power, reactive power, and ramp service are transacted in the real-time market. It is assumed that the distribution system transacts energy and ancillary services with the AMGs. The ADSO can change the topology of its system in normal conditions in a preventive way to reduce the impacts of probable external shocks. Further, the ADSO can determine the location of MESSs to reduce the impacts of probable

Table 2
The number of scenario generation, reduction, and characteristics of AMGs.

sSystem parameter	Value
Number of the scenarios of volumes and prices of day-ahead AMGs active power and ancillary services that are accepted by the ADSO	1000
Number of the scenarios of volumes and prices of day-ahead ADSO active power and ancillary services that are accepted by the wholesale market	1000
Number of the scenarios of day-ahead electrical loads	1000
Number of the scenarios of day-ahead intermittent power generation	1000
Number of the scenarios of smart homes demand response contribution scenarios	1000
Number of the scenarios of ADSO electrical system external shocks	1000
Number of the volumes and prices of day-ahead parking lots active power and ancillary services	1000
Number of the reduced scenarios of volumes and prices of day-ahead AMGs active power and ancillary services that are accepted by the ADSO	10
Number of the reduced scenarios of volumes and prices of day-ahead ADSO active power and ancillary services that are accepted by the wholesale market	10
Number of the reduced scenarios of day-ahead electrical loads	10
Number of the reduced scenarios of day-ahead intermittent power generation	10
Number of the volumes and prices of reduced scenarios of day-ahead parking lots active power and ancillary services	10
Number of the reduced scenarios of smart homes demand response contribution scenarios	10
Number of the reduced scenarios of ADSO electrical system external shocks	10
Maximum active power capacity of AMG that can inject into ADS	**kW**
AMG1	450
AMG2	500
AMG3	580
AMG4	600
AMG5	700
AMG6	720
AMG7	730

Table 3
The characteristics of MESSs.

	Charging/ discharging efficiency	State of charge max/State of charge min	P maximum charging/ P max discharging	Capacity
MESS	0.9	1/0.25	25/20 kW/h	300 kWh

external shocks. In real-time operational scheduling, the ADSO can utilize the switching process in a corrective way to change the system topology and mitigate the impacts of external shocks. It is assumed that each smart home is equipped with a Home Energy Management System (HEMS) that optimally schedules the load commitment. Based on the described framework, a two-stage stochastic optimization process is proposed. As shown in Fig. 2, the optimal scheduling of energy resources for the day-ahead and real-time horizons are determined in the first and second stages, respectively.

The first stage of the optimization problem is compromised three-level processes that are optimized on the day-ahead horizon and in a preventive way to mitigate the impacts of probable external shocks. The first level of the first stage problem finds the optimal topology of the distribution system and the allocating of MESSs in a preventive way to reduce the probable external shock. The ADSO switches the normally opened/closed switches to reconfigure the system and mitigate the estimated shocks. The second level problem optimizes the scheduling problem of the AMGs for the day-ahead horizon. The third level problem optimizes the ADSO DERs day-ahead scheduling considering the AMGs energy and ancillary services transactions. The real-time problem is categorized into the normal state real-time optimization problem and shock conditions real-time optimization problem. If there is not any shock condition, the real-time optimization problem compromises the optimization process of the AMGs and ADSO in the first and second stages, respectively. If there is an external shock condition, the first level of the second stage problem determines the optimal topology of the distribution system in a corrective way to reduce the external shock. The ADSO switches the normally opened/closed switches to reconfigure the system and mitigate the estimated shocks. The second and third-level problems determine the optimal scheduling of the AMGs and ADSO for the real-time horizon.

2.1. The Day-Ahead Optimization Problems

As shown in Fig. 2, at the first stage problem, the day-ahead optimization process compromises three levels: 1) The ADSO day-ahead topology and MESS allocation optimization problem (first level of the first stage problem), 2) the AMGs day-ahead problem (second level of the first stage problem); 3) and the ADSO day-ahead optimization problem (third level of the first stage). The first stage optimization process is described in the following subsections.

2.1.1. The ADSO day-ahead topology and MESS allocation optimization problem (first level of the first stage problem)

The first level of the first stage optimization problem explores the system conditions in the probable external shock conditions. The ADSO simulates the impacts of external shocks on its system to determine the estimated volume of critical loads that are not supplied. Then, the ADSO determines the optimal sectionalizing process of its system into multi-

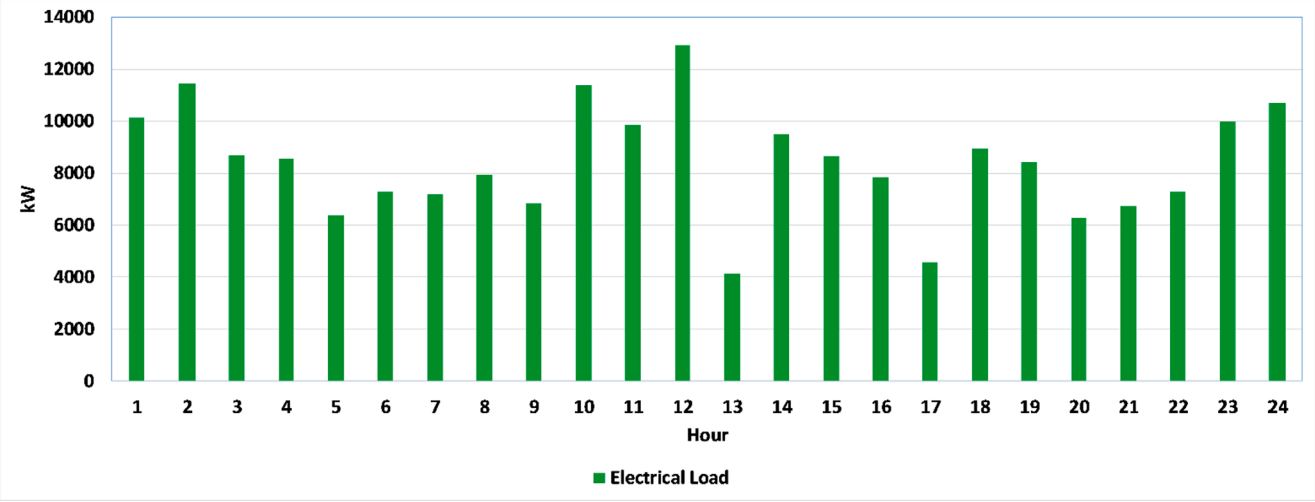

Fig. 5. The day-ahead forecasted electrical load for one of the reduced scenarios.

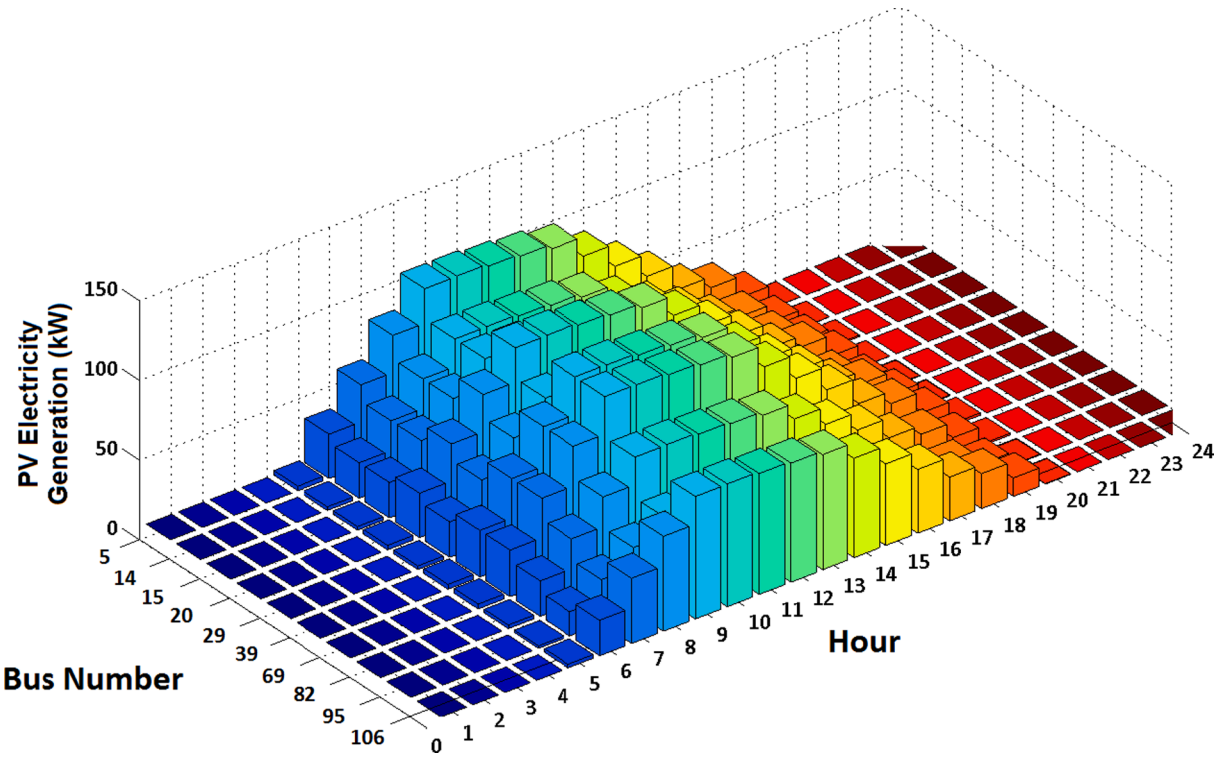

Fig. 6. The forecasted photovoltaic systems electricity generation for one of the reduced scenarios.

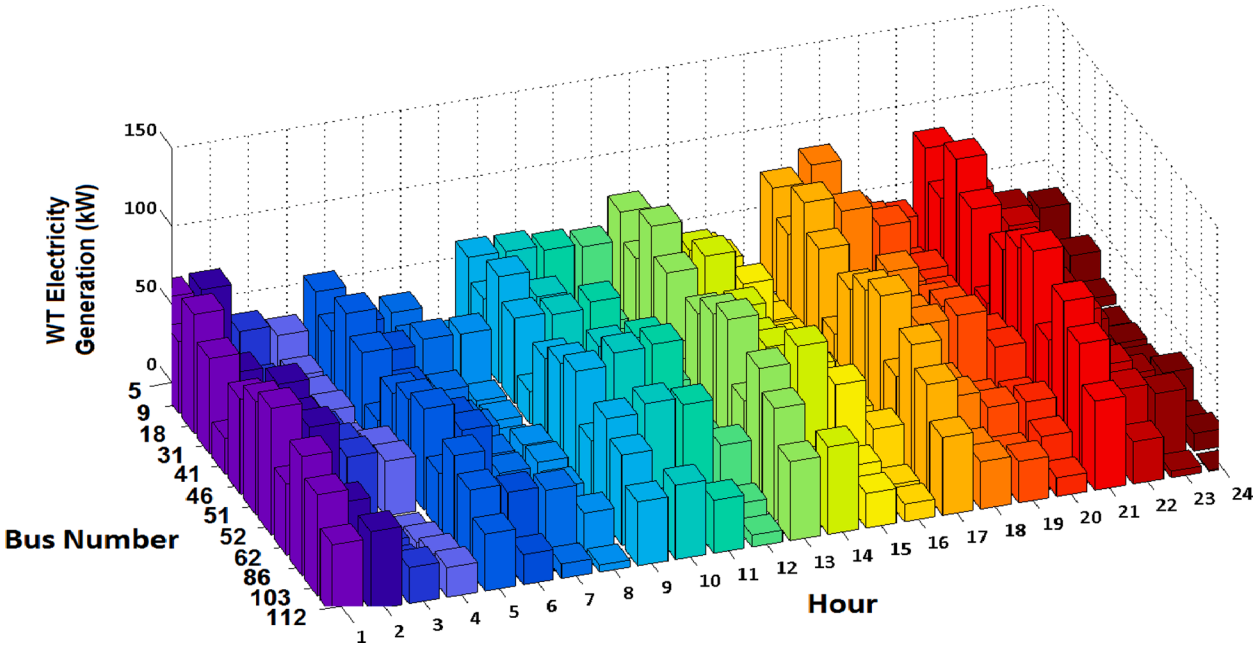

Fig. 7. The forecasted wind turbine electricity generation for one of the reduced scenarios.

zones to reduce the impacts of the external shocks in a preventive way. Further, the ADSO allocates the MESSs for reducing the impacts of probable external shocks. Then, the second and third levels of the first stage optimization process are carried out. The volume of the probable load shedding is determined more precisely in the third level of the first stage problem. At the third level, if the volume of the Self-Healing Index (SHI) is less than a predefined threshold, the first level of the first stage problem is resolved and the formation of microgrids is changed. Then, the second and third-level optimization processes are solved again and the condition of the electricity supply of critical loads is explored. If the critical loads are not supplied, the optimization process of the third-level changes is carried out again. At the first level of the first stage level, it is assumed that all of the dispatchable distributed energy resources are available and the uncertainties of intermittent electricity generation facilities are not considered. This level estimates the unserved non-critical load and determines the topology of the system.

The objective function of the first level of the first stage system can be written as (1):

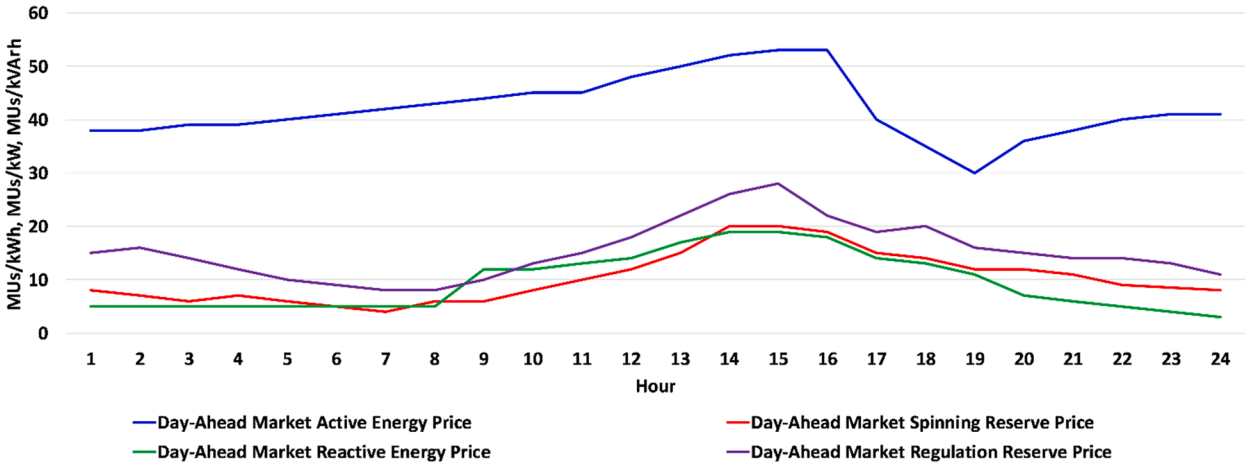

Fig. 8. The day-ahead forecasted price of the active power and ancillary services for one of the reduced scenarios.

$$Min\ \mathbb{F}_1^{\mathrm{DA}} = \sum_{\mathrm{EXSS}} \mathrm{prob}\cdot\left(-\mathrm{W}_1\cdot\mathrm{SHI} + \mathrm{W}_2\cdot\sum_{\mathrm{NSW}}\mathrm{X} + \mathrm{W}_3\cdot\sum_{\mathrm{NMESS}}\mathrm{Z}\cdot\mathrm{C}_{\mathrm{MESS}}\right) \quad (1)$$

Where, *EXSS* is the set of the probable external shock scenarios. Eq. (1) compromises the self-healing index (SHI), boundary lines of microgrids, and allocating costs of MESSs. DA stands for day-ahead. The first term of objective function maximizes the *SHI*. The second term of the objective function minimizes the electricity flow in the boundary line (*X*). It is assumed that the lines of the distribution system are equipped with the normally closed switches and these switches can be opened in external shock conditions to sectionalize the distribution system into multi-zones. Further, the *Y* variable presents the served non-critical load and the optimization process curtails this load in contingent conditions. The third term of (1) minimizes the allocating costs of MESSs. Further, the *Z* variable presents the binary decision variable for allocating of MESSs in the available locations. C_{MESS} is the aggregated operational and transportation costs of MESS.

W_1, W_2, and W_3 are weighting factors. The self-healing index is defined as (2):

$$SHI = \frac{\sum P^{CL}|_{External\_Shock} + \sum Y\cdot P^{NCL}\cdot D|_{External\_Shock}}{\sum P^{CL}|_{Normal\_Condition} + \sum P^{NCL}|_{Normal\_Condition}} \quad (2)$$

The *D* variable presents the duration of deferrable non-critical load commitment. Eq. (2) calculates the ratio of the aggregated served critical loads and dispatched non-critical loads in the external shock conditions concerning their aggregated values in the normal operational conditions.

The constraints of the first level of the first stage compromise the following constraints.

The electric power balance constraint for the ADS is given by (3):

$$P^{ADS} = \left(\sum P^{CHP} \mp \sum P^{SH} + \sum P^{WT} + \sum P^{PV} \mp \sum P^{PL} - \sum P^{CL} - \sum Y\cdot P^{NCL}\cdot D + \sum P^{DG} \mp \sum P^{ESS} + \sum P^{MESS} \mp \sum P^{AMGTRANS} - P^{ADSLoss} \mp \sum P^{WMTRANS}\right) \quad (3)$$

Where, P^{CHP}, P^{SH}, P^{WT}, P^{PV}, P^{PL}, P^{CL}, P^{NCL},P^{DG}, P^{ESS}, P^{MESS}, $P^{AMGTRANS}$,$P^{ADSLoss}$, $P^{WMTRANS}$ are active power of CHP, smart home, wind turbine, photovoltaic array, parking lot, critical load, non-critical load, distributed generation facility, energy storage, MESS, the transaction with AMGs, active power loss, the transaction with the wholesale market, respectively. The AC load flow constraints are considered in the optimization process and are not presented for the sack of space [1].

The ADSO system is constrained by the static security constraints that can be presented as (4) and (5):

$$\sqrt{P^2_{ADS\_LINE} + Q^2_{ADS\_LINE}} \leqslant F^{\mathrm{Max}}_{ADS\_LINE} \quad (4)$$

$$V^{\min} \leqslant |V| \leqslant V^{\max} \quad (5)$$

Eq. (4) terms are active (P_{ADS_LINE}) and reactive power (Q_{ADS_LINE}) of the ADS feeders. $F^{Max}_{ADS\_LINE}$ is the maximum flow limit of the ADS feeder. Eq. (5) presents the limits of the ADS bus voltage.

The electricity generation constraints of DGs, PVs, WTs, CHPs, and their ramp rates are considered in the optimization process. Further, the following constraints of ESSs and MESSs are considered in the optimization process: the state of charge of energy storage constraints, simultaneous charge and discharge constraints, and the maximum charge limits constraints.

2.1.2. The day-ahead AMGs optimization problem (second level of the first stage problem)

The microgrids can submit their bids to the ADS database for the day-ahead energy and ancillary service markets. It is assumed that the AMGs maximize their profits in the day-ahead energy and ancillary service markets. The general form of the objective function of the day-ahead optimization process of AMGs can be written as (6):

$$Max\ \mathbb{F}^{\mathrm{DA}}_{\mathrm{AMGs}} = \sum_{\Xi} \mathrm{prob}\cdot\left(\lambda^{\mathrm{SR\_DA}}_{\mathrm{AMG}}\cdot\mathrm{SR}^{\mathrm{DA}}_{\mathrm{AMG}} + \lambda^{\mathrm{AP\_DA}}_{\mathrm{AMG}}\cdot\mathrm{P}^{\mathrm{DA}}_{\mathrm{AMG}} + \lambda^{\mathrm{RP\_DA}}_{\mathrm{AMG}}\cdot\mathrm{Q}^{\mathrm{DA}}_{\mathrm{AMG}} + \lambda^{\mathrm{RR\_DA}}_{\mathrm{AMG}}\cdot\mathrm{RR}^{\mathrm{DA}}_{\mathrm{AMG}} - C^{DA}_{AMG} - \sum Penalty\right) \quad (6)$$

Where, Ξ is the set of the operating state scenarios of AMGs. In (6), $\lambda^{SR\_DA}_{AMG}$, $\lambda^{AP\_DA}_{AMG}$, $\lambda^{RP\_DA}_{AMG}$, $\lambda^{RR\_DA}_{AMG}$ are the submitted values of the day-ahead spinning reserve price, active power price, reactive power, and regulating reserve price, respectively. The $SR^{DA}_{AMG}, P^{DA}_{AMG}, Q^{DA}_{AMG}, RR^{DA}_{AMG}$ variables are the day-ahead accepted values of AMGs spinning reserve, active power, reactive power, and regulating reserve, respectively. The values of $SR^{DA}_{AMG}, P^{DA}_{AMG}, Q^{DA}_{AMG}, RR^{DA}_{AMG}$ variables are functions of the ADS conditions in the external shocks, the ADS topology, the MESSs allocating, and the available dispatchable energy resources of ADS. The C^{DA}_{AMG} is the day-ahead operating cost of AMG.

Eq. (6) consists of the following terms: 1) the revenue of spinning reserve sold to the ADS Operator (ADSO) ($\lambda^{SR\_DA}_{AMG}\cdot SR^{DA}_{AMG}$); 2) the revenue of active power sold to the ADSO ($\lambda^{AP\_DA}_{AMG}\cdot P^{DA}_{AMG}$); 3) the revenue of reactive power sold to the ADSO ($\lambda^{RP\_DA}_{AMG}\cdot Q^{DA}_{AMG}$); 4) the revenue of regulating reserve sold to the ADSO ($\lambda^{RR\_DA}_{AMG}\cdot RR^{DA}_{AMG}$) ; 5) the operating costs (C^{DA}_{AMG}); 6) and the penalties of mismatches.

It is assumed that the AMGs have a communication infrastructure and can coordinate their bidding strategies using the proposed optimi-

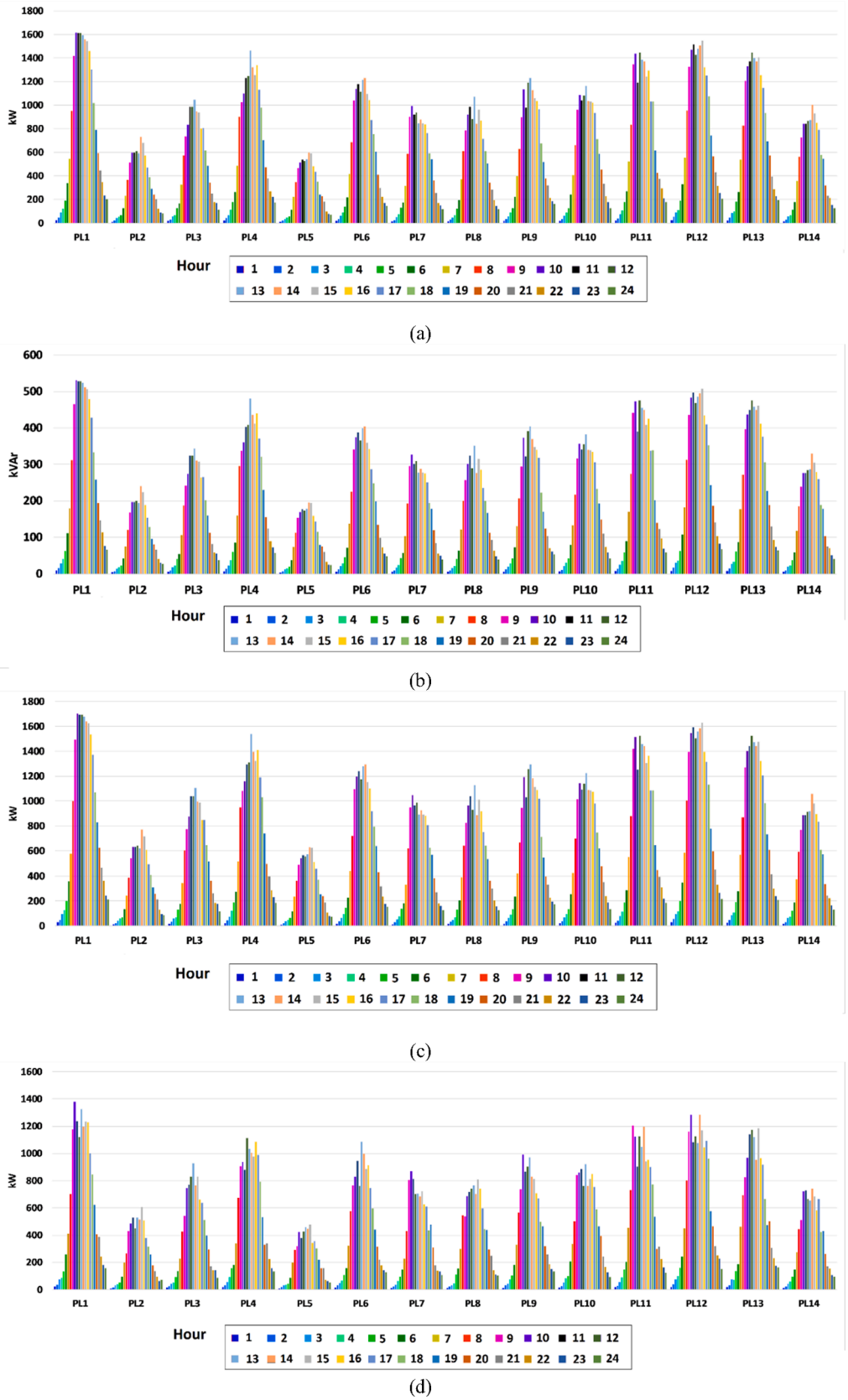

Fig. 9. (a) The dispatched values of active power, (b) The dispatched values of reactive power, (c) The dispatched values of spinning reserve, (d) The dispatched values of regulating reserve of parking lots for the day-ahead market.

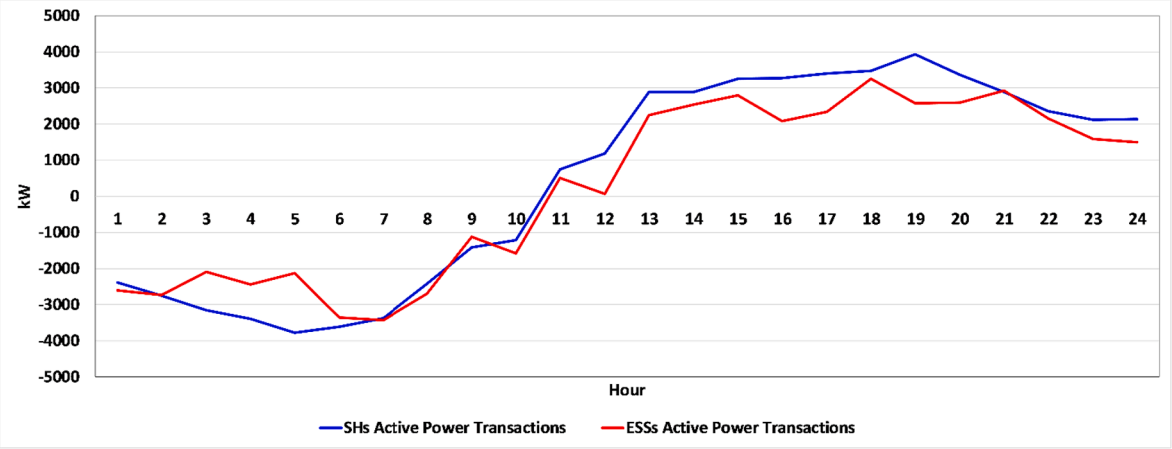

Fig. 10. The dispatched values of the active power of smart homes and energy transactions of ESSs.

zation process. When the AMGs do not coordinate their bidding strategies, their submitted values of the day-ahead spinning reserve price, active power price, reactive power, and regulating reserve price may be lower than the coordinated bidding case base on the fact that the ADSO endeavors to purchase these commodities with the lowest price. However, the AMGs can coordinate their bids to increase their submitted price and gain more profit. Hence, the proposed optimization process determines the optimal values of $SR^{DA}_{AMG}, P^{DA}_{AMG}, Q^{DA}_{AMG}, RR^{DA}_{AMG}$ variables for the coordinated bidding strategies of AMGs.

Eq. (6) is subject to the following constraints:

The minimum and maximum limits of electricity generation of facilities, the ramp rate constraints of electricity generation units that are available in [1], and not presented for the sack of space.

The Coordination Gain index (CGI) is proposed to assess the impacts of coordinated bidding of AMGs as (7):

$$CGI = \frac{\mathbb{F}^{\mathrm{DA}}_{\mathrm{AMGs\ CB}} - \mathbb{F}^{\mathrm{DA}}_{\mathrm{AMGs\ UB}}}{\mathbb{F}^{\mathrm{DA}}_{\mathrm{AMGs\ UB}}} \tag{7}$$

$\mathbb{F}^{\mathrm{DA}}_{\mathrm{AMGs\ CB}}$ is the objective function of AMGs when they coordinate their biddings. Further, $\mathbb{F}^{\mathrm{DA}}_{\mathrm{AMGs\ UB}}$ is the objective function of AMGs when they do not coordinate their biddings.

2.1.3. The ADSO day-ahead optimization problem (third level of the first stage problem)

The ADSO transacts active power and ancillary service markets with the wholesale electricity market. At this level, the scenarios of day-ahead values of ADSO active power and ancillary services prices are generated and reduced.

The ADSO day-ahead optimization process can be written as (8):

$$\begin{aligned} Max\ \mathbb{F}^{\mathrm{DA}}_{\mathrm{ADSO}} = & \sum_{\mathrm{ADSNS}} \mathrm{prob}\cdot \mathrm{W}_4\cdot(\lambda^{\mathrm{AP\_DA}}_{\mathrm{ADSO}}\cdot \mathrm{P}^{\mathrm{DA}}_{\mathrm{ADSO}} + \lambda^{\mathrm{RP\_DA}}_{\mathrm{ADSO}}\cdot \mathrm{Q}^{\mathrm{DA}}_{\mathrm{ADSO}}) + \mathrm{W}_5\cdot\mathbb{F}^{\mathrm{DA}}_{1} \\ & - \mathrm{W}_6\cdot\mathbb{F}^{\mathrm{DA}}_{\mathrm{AMGs}} - \sum_{DERNS} prob\cdot W_7\cdot(C^{DA}_{CHP} + C^{DA}_{DG} + C^{DA}_{ESS} \\ & + C^{DA}_{DRP\_PSH} + C^{DA}_{ASH} + C^{DA}_{PL} + C^{DA}_{WT} + C^{DA}_{PV} + C^{DA}_{Purchase\_WM} \\ & + \sum Penalty) + \sum_{\Xi} prob\cdot W_8\cdot CGI \end{aligned} \tag{8}$$

Where, *ADSNS* is the set of the normal operating scenarios of the ADSO. The parameters $\lambda^{AP\_DA}_{ADSO}, \lambda^{RP\_DA}_{ADSO}$ are the submitted values of the ADSO day-ahead spinning active power price and reactive power price, respectively. The $P^{DA}_{ADSO}, Q^{DA}_{ADSO}$ variables are the day-ahead accepted value of ADSO active power and reactive power, respectively. *DERNS* is the set of the normal operating scenarios of the ADSO DERs. W_4, W_5, W_6, and W_7 are weighting factors.

Eq. (8) consists of the following terms: 1) the revenue of active power sold to the wholesale electricity market ($\lambda^{AP\_DA}_{ADSO}\cdot P^{DA}_{ADSO}$); 2) the revenue of reactive power sold to the wholesale electricity market ($\lambda^{RP\_DA}_{ADSO}\cdot Q^{DA}_{ADSO}$); 3) the $\mathbb{F}^{\mathrm{DA}}_{1}$ term is the first level of the first stage objective function that is minimized at this level considering the available distributed energy resources and the uncertainties of system parameters; 4) the $\mathbb{F}^{\mathrm{DA}}_{\mathrm{MGs}}$ term is the second level of the first stage objective function; 5) the operating cost of CHPs; 6) the operating cost of DGs; 7) the operating cost of ESSs; 8) the demand response costs of passive smart homes; 9) the costs of active smart home contributions; 10) the operating costs pf parking lots; 11) the operating costs of WTs; 12) the operating costs of PVs; 13) the costs of active and reactive power purchased from the wholesale market; 14) the penalties of mismatches of active and reactive power sold to the wholesale market; 15) and the sum of the coordination gain index.

Eq. (8) is subjected to the same constraints as Eq. (1).

2.2. The Real-Time Optimization Problems

As shown in Fig. 2, the real-time problem compromises the normal state and shock conditions optimization problems. If there is not any shock condition, the real-time problems compromise AMGs and ADSO optimization problems for the real-time horizon that are solved in the first and second levels, respectively. If there is an external shock condition, the first level of the second stage problem determines the optimal topology of the distribution system in a corrective way to reduce the external shock. The ADSO switches the normally opened/closed switches to reconfigure the system and mitigate the estimated shocks. The second and third-level problems determine the optimal scheduling of AMGs and ADSO, respectively. Thus, the real-time optimization process is categorized into: 1) normal state conditions, and 2) external shock conditions.

A. Real-Time Optimization Process for Normal State Conditions

2.2.1. The AMGs real-time normal state optimization problem (first level of the second stage normal state problem)

It is assumed that the AMG owner can participate in the real-time ramp market to maximize his/her profits. The objective function of AMG in the real-time market can be written as (9):

$$\begin{aligned} Max\ \mathfrak{N}^{\mathrm{RT}}_{\mathrm{AMG}} = & \sum\nolimits_{t=0}^{\mathrm{T}} (\lambda^{\mathrm{AP\_RT}}_{\mathrm{AMG}}\cdot \mathrm{P}^{\mathrm{RT}}_{\mathrm{AMG}} + \lambda^{\mathrm{RAMP^+}}_{\mathrm{AMG}}\cdot \mathrm{P}^{\mathrm{RAMP^+}}_{\mathrm{AMG}} + \lambda^{\mathrm{RAMP^-}}_{\mathrm{AMG}}\cdot \mathrm{P}^{\mathrm{RAMP^-}}_{\mathrm{AMG}} \\ & - \mathrm{c}^{\mathrm{RT}}_{\mathrm{AMG}}\cdot \mathrm{P}^{\mathrm{RT}}_{\mathrm{AMG}} - c^{RAMP^-}_{AMG}\cdot P^{RAMP^-}_{AMG} \\ & - c^{RAMP^+}_{AMG}\cdot P^{RAMP^+}_{AMG} - \sum Penalty) \end{aligned} \tag{9}$$

Where, $\lambda^{AP\_RT}_{AMG}, \lambda^{RAMP^+}_{AMG}, \lambda^{RAMP^-}_{AMG}$ are the submitted values of AMG real-time market active power price, ramp-up price, and ramp-down price, respectively. RT stands for real-time. The P^{RT}_{AMG} variable is the accepted

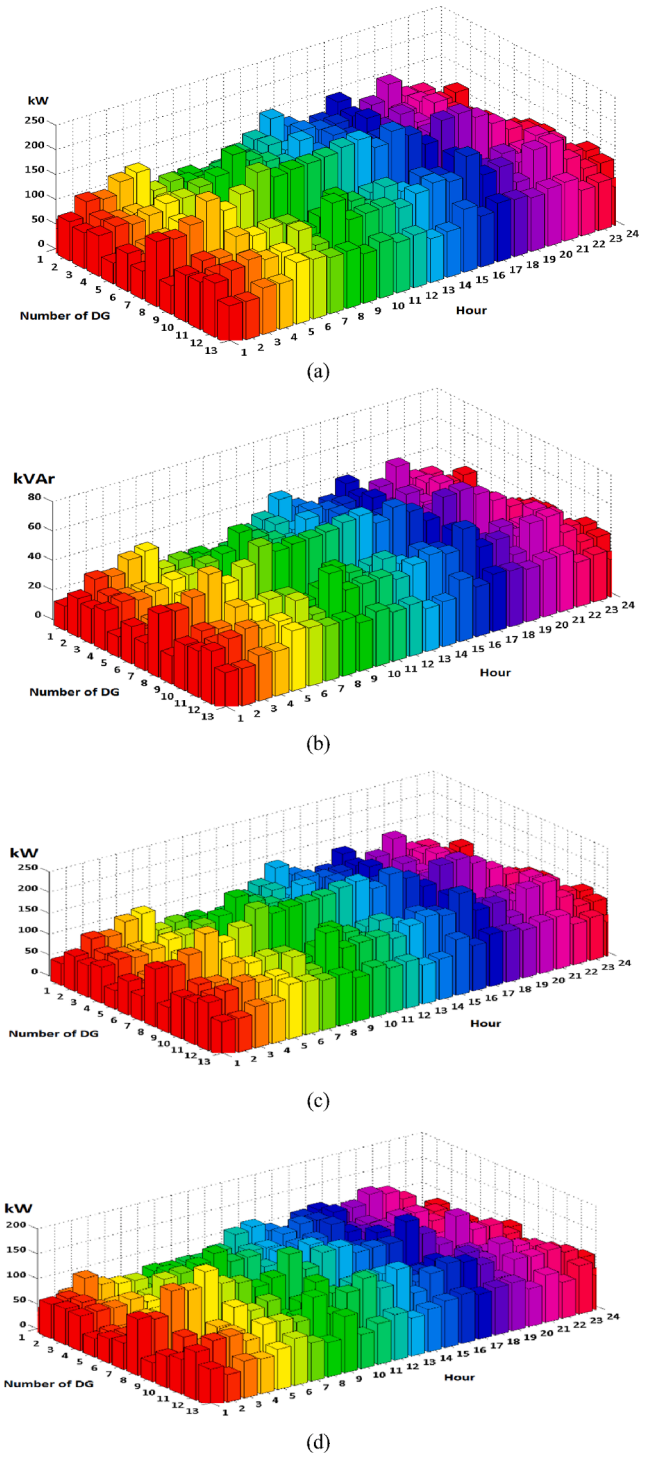

Fig. 11. (a) The dispatched values of active power, (b) The dispatched values of reactive power, (c) The dispatched values of spinning reserve, and (d) The dispatched values of regulating reserve of distributed generation facilities for the day-ahead market.

value of AMG active power generation in the real-time market. The $P_{AMG}^{RAMP^+}$, $P_{AMG}^{RAMP^-}$ variables are the accepted values of AMG ramp-up and ramp-down active power volumes, respectively. The parameters c_{AMG}^{RT}, $c_{AMG}^{RAMP^+}$, $c_{AMG}^{RAMP^-}$ are the AMG electricity generation cost in the real-time market, ramp-up cost, and ramp-down cost, respectively.

Eq. (9) compromises the following terms: 1) the revenue of active power sold to the parking lot ($\lambda_{AMG}^{AP\_RT} \cdot P_{AMG}^{RT}$); 2) the revenue of ramp-up ancillary service sold to the parking lot ($\lambda_{AMG}^{RAMP^+} \cdot P_{AMG}^{RAMP^+}$); 3) the revenue of ramp-down ancillary service sold to the parking lot ($\lambda_{AMG}^{RAMP^-} \cdot P_{AMG}^{RAMP^-}$); 4) the cost of active power generation ($c_{AMG}^{RT} \cdot P_{AMG}^{RT}$); 5) the cost of ramp-down ancillary service ($c_{AMG}^{RAMP^-} \cdot P_{AMG}^{RAMP^-}$); 6) the cost of ramp-up ancillary service ($c_{AMG}^{RAMP^+} \cdot P_{AMG}^{RAMP^+}$); 7) the penalties of mismatches ($\sum Penalty$).

Eq. (9) is subjected to the second level of the first stage problem constraints.

2.2.2. The ADSO real-time normal state optimization problem (second level of the second stage normal state problem)

The ADSO transacts active power and ancillary service markets with the real-time wholesale electricity market. The objective function of the real-time optimization process of ADSO in normal operating conditions is presented as (10):

$$\begin{aligned} Max\ \mathfrak{W}_{ADSO}^{RT\_NORMAL} = \sum_{t=0}^{T} W_1^{'} \cdot (\lambda_{ADSO}^{AP\_RT} \cdot P_{ADSO}^{RT} + \lambda_{ADSO}^{RP\_RT} \cdot Q_{ADSO}^{RT} - C_{CHP}^{RT} \\ - C_{DG}^{RT} - C_{ESS}^{RT} - C_{DRP\_PSH}^{RT} - C_{ASH}^{RT} - C_{PL}^{RT} - C_{WT}^{RT} \\ - C_{PV}^{RT} - C_{Purchase\_WM}^{RT} - \sum Penalty) - W_2^{'} \cdot \mathfrak{W}_{MG}^{RT} \end{aligned} \tag{10}$$

Where, $\lambda_{ADSO}^{AP\_RT}$, $\lambda_{ADSO}^{RP\_RT}$ are the submitted values of the ADSO real-time market active power price and reactive power price, respectively. The P_{ADSO}^{RT}, Q_{ADSO}^{RT} variables are the accepted value of the ADSO real-time market active power and reactive power, respectively. $W_1^{'}$ and $W_2^{'}$ are weighting factors.

Eq. (10) consists of the following terms: 1) the revenue of active power sold to the wholesale market ($\lambda_{ADSO}^{AP\_RT} \cdot P_{ADSO}^{RT}$); 2) the revenue of reactive power sold to the wholesale market ($\lambda_{ADSO}^{RP\_RT} \cdot Q_{ADSO}^{RT}$); 3) the operating cost of CHPs; 4) the operating cost of DGs; 5) the operating cost of ESSs; 6) the demand response costs of passive smart homes; 7) the costs of active smart home contributions; 8) the operating costs of parking lots; 9) the operating costs of WTs; 10) the operating costs of PVs; 11) the costs of active and reactive power purchased from the wholesale market; 12) the penalties of mismatches of active and reactive power sold to the wholesale market; 13) and the $\mathfrak{W}_{MG}^{RT}$ term is the first level of the second stage objective function. Eq. (10) is subjected to the first level of the first stage problem constraints.

B. Real-Time Optimization Process for External Shock Conditions

In real-time operating conditions, the ADSO checks the system status. If the shock state is detected, the ADSO can change the topology of the distribution system to mitigate the impact of external shock. The real-time optimization process for external shock conditions compromises four levels. The first level of the second stage problem reads the day-ahead optimal topology database and determines the optimal topology of the distribution system to reduce the external shock. The second and third-level problems determine the optimal scheduling of AMGs and ADSO, respectively. The second-stage optimization process for the shock state compromises the following problems.

2.2.3. The optimal switching of the distribution system (first level of the second stage shock state problem)

In external shock conditions, the ADSO changes its system topology. The first level of the second stage shock state reads from the first level of the first stage problem database. Thus, the objective function of this problem can be written as (11):

$$Min\ \mathbb{Z}_{1\ ADSO}^{RT\_SHOCK} = W_1^{''} \cdot \sum_{NL} CIC \cdot (1 - Y) + W_2^{''} \cdot \sum_{NSW} X \tag{11}$$

Where, NL is the set of the system loads. Eq. (11) compromises the Customer Interruption Cost (CIC) of unserved load and boundary lines of the system. $W_1^{''}$ and $W_2^{''}$ are weighting factors. Eq. (11) constraints are the same as Eq. (1) constraints.

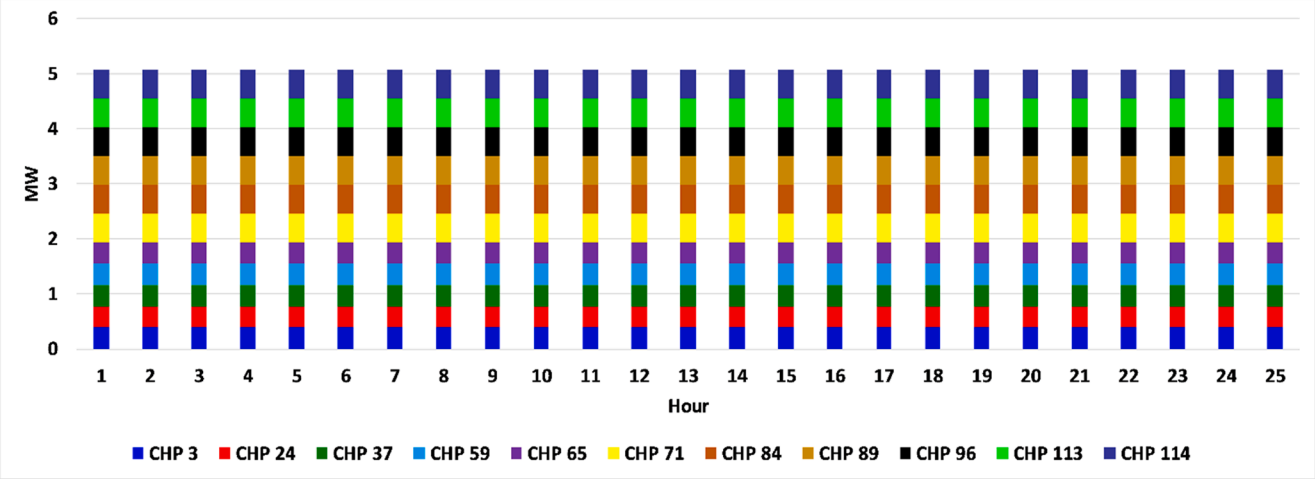

Fig. 12. The active power generation of CHP facilities for the day-ahead market.

2.2.4. The AMGs real-time shock state optimization problem (second level of the second stage shock state problem)

It is assumed that AMG endeavors to maximize its profits in the real-time ramp market. The objective function of AMG for the second level of the second stage shock state problem can be written as (12):

$$Max\ \mathbb{Z}_{AMG}^{RT\_SHOCK} = \mathfrak{W}_{\mathrm{AMG}}^{\mathrm{RT}} \tag{12}$$

Eq. (12) is subjected to Eq. (9) problem constraints.

2.2.5. The real-time shock state ADSO Optimization Problem (third level of the second stage shock state problem)

At this optimization level, it is assumed that the distribution system can be categorized into normal state zones and shock state zones. The ADSO can transact active power and ancillary service markets with the wholesale electricity market in the real-time market for the normal state zones. The ADSO should minimize the not-served loads; energy purchased costs, and operating costs of the system in shock state zones; meanwhile, maximize the profit of active and reactive powers sold to the wholesale market for the normal state zones. Thus, the objective function of the real-time optimization process of ADSO for the shock state conditions can be written as (13):

$$\begin{aligned} Min\ \mathbb{Z}_{2\ ADSO}^{RT\_SHOCK} = & -W_3'' \cdot \mathbb{Z}_{AMG}^{RT\_SHOCK} + \sum\nolimits_{t=0}^{T} W_4'' \cdot (\lambda_{ADSO}^{AP\_RT} \cdot P_{ADSO}^{RT} \\ & + \lambda_{ADSO}^{RP\_RT} \cdot Q_{ADSO}^{RT} - C_{CHP}^{RT} - C_{DG}^{RT} - C_{ESS}^{RT} - C_{DRP\_PSH}^{RT} \\ & - C_{ASH}^{RT} - C_{PL}^{RT} - C_{WT}^{RT} - C_{PV}^{RT} - C_{Purchase\_WM}^{RT} - \sum Penalty \\ & + W_5'' \cdot \sum_{NL} CIC \cdot (1 - Y)) \end{aligned} \tag{13}$$

W_3'', W_4'', and W_5'' are weighting factors. Eq. (13) terms are presented in Eq. (11) and Eq. (12). Eq. (13) is subjected to Eq. (9) constraints.

3. Solution Methodology

As shown in Fig. 3, the proposed algorithm is an iterative two-stage optimization problem. The optimization process has the following assumptions:

- The demand response process performs direct load control to commit the non-critical loads.
- The proposed optimization problem is subjected to the following sources of uncertainty: 1) the volumes and prices of day-ahead AMGs active power and ancillary services that are accepted by the ADSO; 2) the volumes and prices of day-ahead ADSO active power and ancillary services that are accepted by the wholesale market; 3) the day-ahead electrical loads; 4) the day-ahead intermittent power generation; 5) the smart homes demand response contribution scenarios; 6) and the ADSO electrical system external shocks.
- The scenario generation and reduction processes are used to carry out the simulation process of stochastic parameters of uncertainties and each uncertain parameter is modeled as a stochastic process. The stochastic process can be represented as its corresponding probability distribution functions [1]. Then, the scenario generation process is utilized to discretize the distribution functions. Finally, each objective function is transformed into random variables, and the expected value of the objective function is calculated. The bidding process of AMGs is carried out using the proposed objective functions to maximize the profit of AMGs. The curse of dimensionality of the generated scenarios may lead to computational problems. Thus, the scenario reduction method should be performed. The forward selection algorithm proposed in [1] is used to reduce the scenarios. Then, the Auto-Regressive Integrated Moving Average (ARIMA) models are utilized to model the (1-5) uncertainties and the Monte Carlo procedure estimates the location and intensity of the external shocks [1,25]. Finally, the scenario reduction process is performed [1,25].
- The weighted sum method is utilized to aggregate the proposed objective functions in the context of a multi-objective optimization program [26].
- All of the non-linear AC load flow is linearized using the proposed method [27].
- The objective functions and their constraints are linearized. The detailed method of the linearization process is presented in [27].
- The weighted sum algorithm is employed to recast the proposed objective functions into multi-objective optimization programs. The detailed model of the weighted sum method is described in [1] and is not presented for the sack of space.
- The algorithm codes were developed in GAMS and MATLAB. The linearized day-ahead and real-time optimization problems are MILP procedures that are solved by the CPLEX solver.

4. Simulation Results

The 123-bus IEEE test system was considered to assess the model [24]. The system comprises thirteen DGs, eleven CHPs, ten photovoltaic systems, twelve wind turbines, fourteen parking lots, and seven AMGs. Fig. 4 presents the topology of the 123-bus IEEE test system. The technical and cost information of CHP units, ESSs, and PV units are presented in [1,24]. The simulation was carried out on a PC (AMD A10-5750M processor, 4*2.5 GHz, 8 GB RAM). The maximum simulation time for

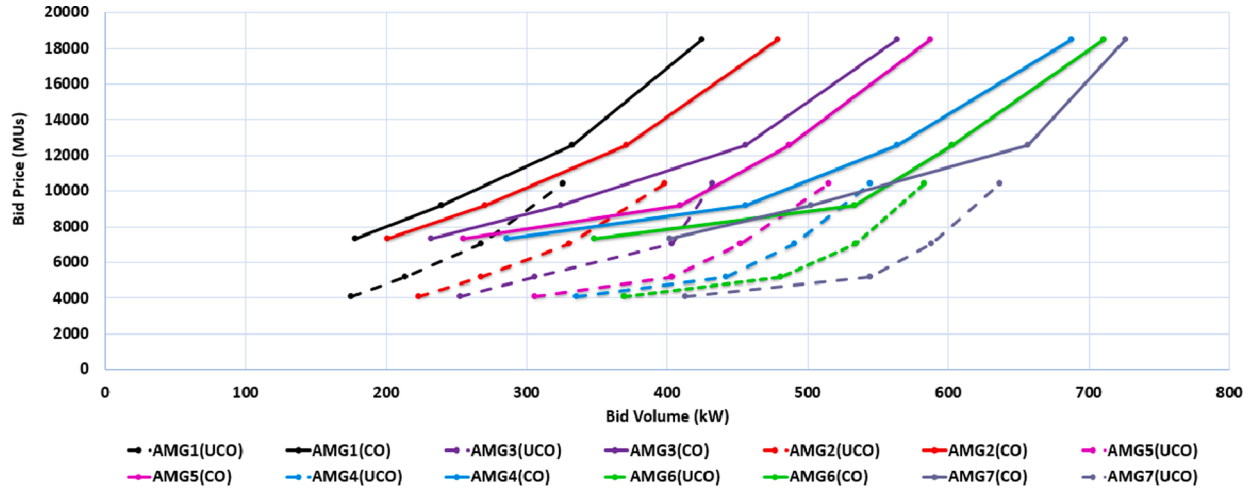

(a)

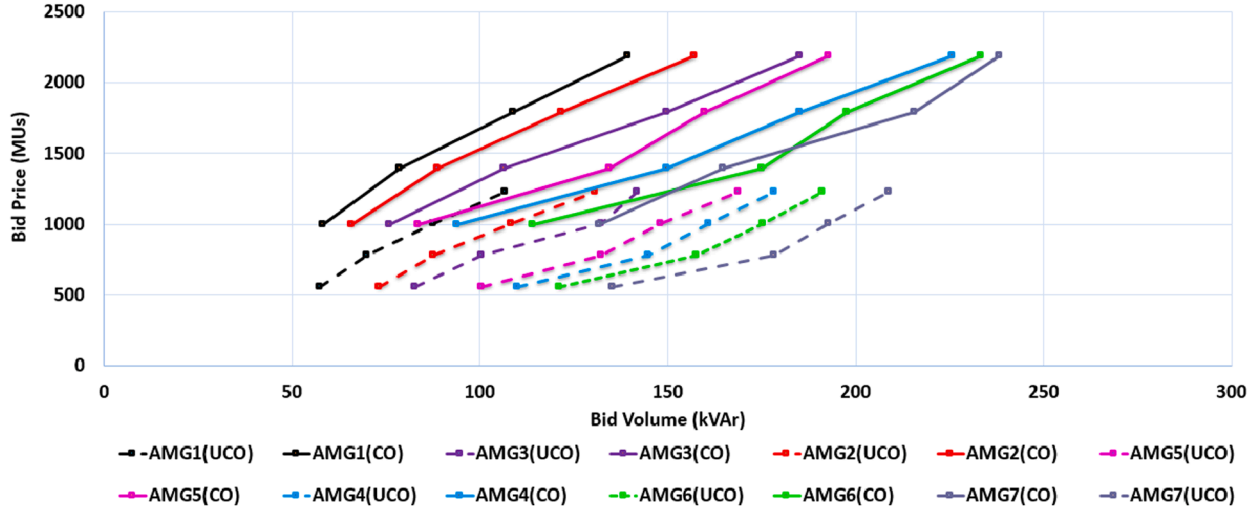

(b)

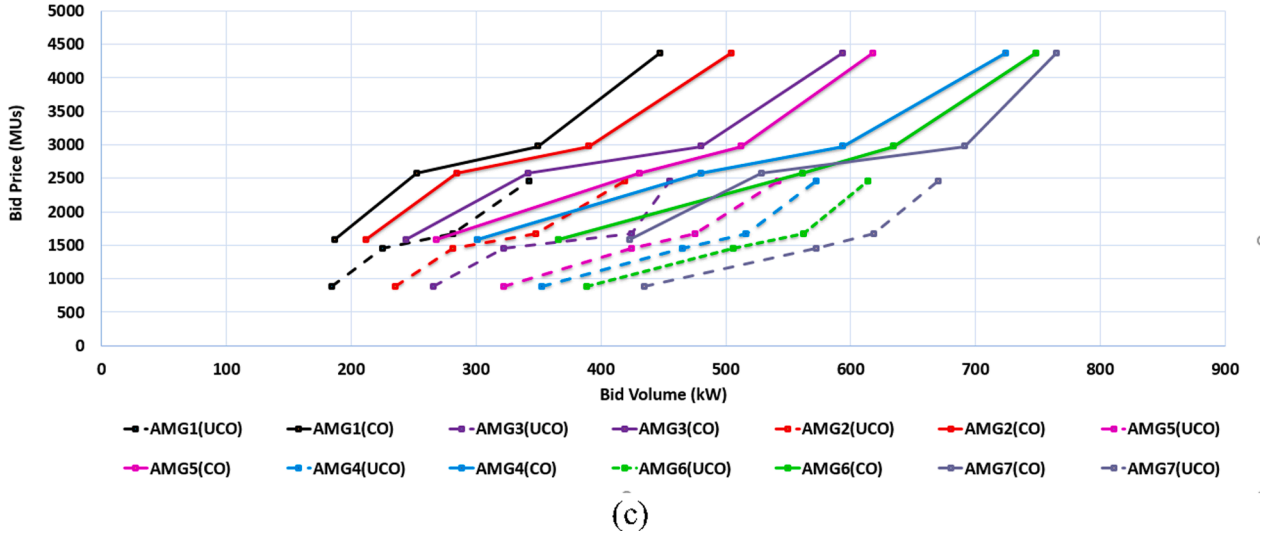

(c)

Fig. 13. The submitted values of coordinated and uncoordinated AMGs' of (a) active power, (b) reactive power, (c) spinning reserve, and (d) regulating reserve.

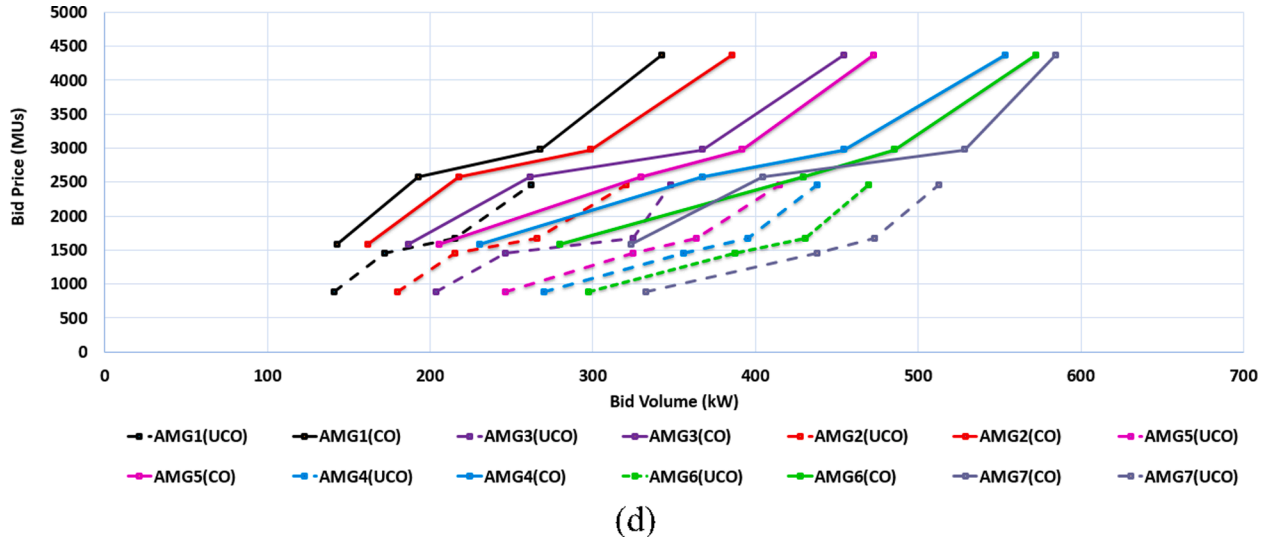

(d)

Fig. 13. (*continued*).

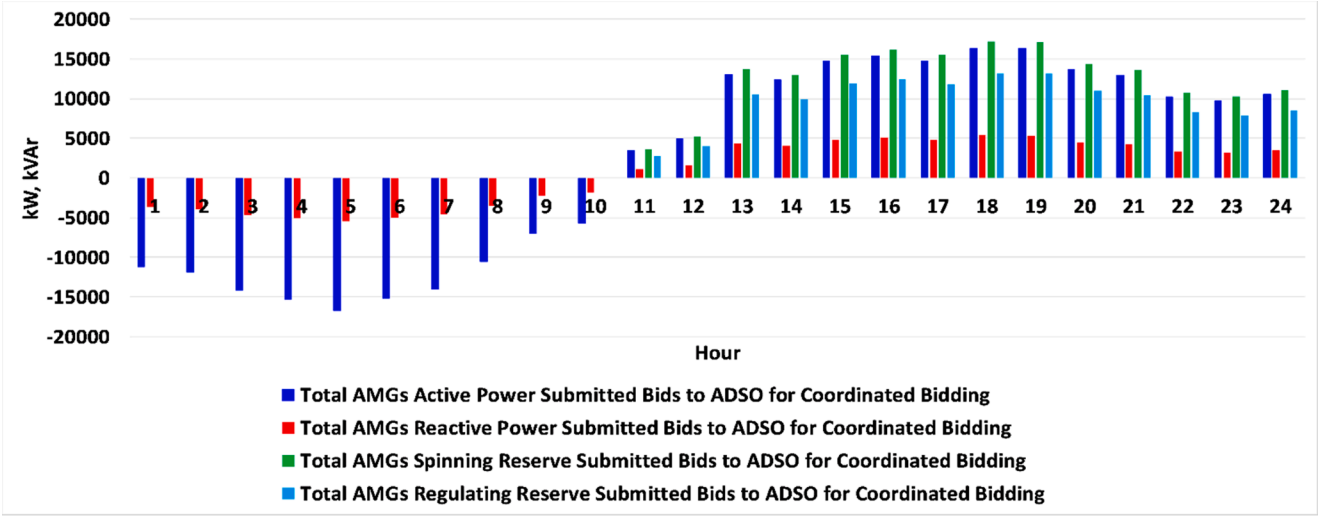

(a)

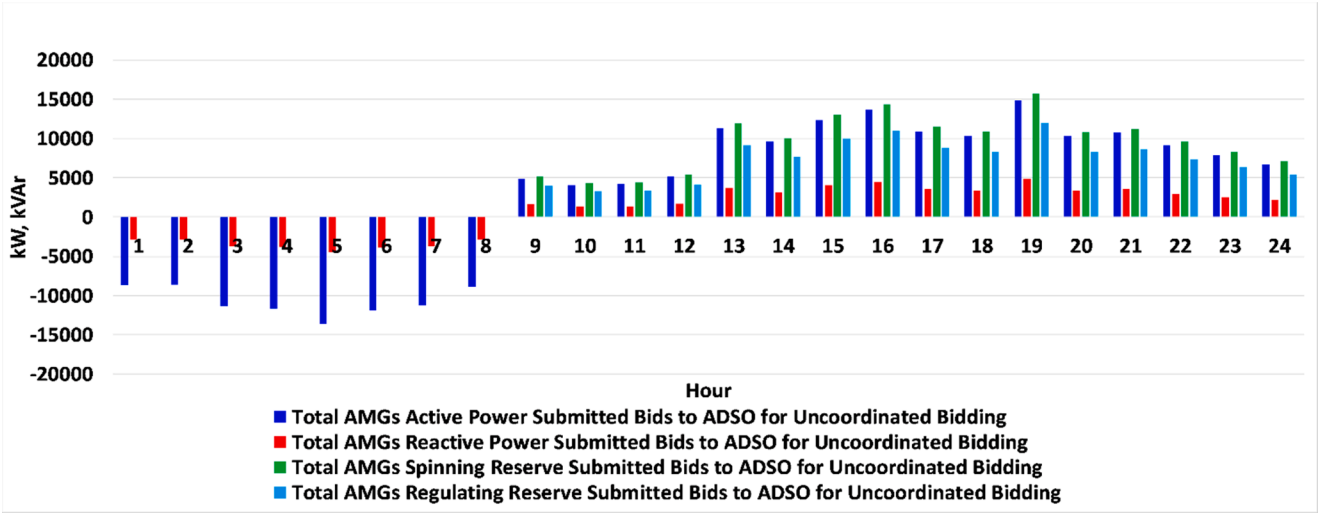

Fig. 14. (a) The aggregated active power, reactive power, spinning reserve, and regulating reserve submitted bids of AMGs for the day-ahead market considering the coordinated biddings of AMGs. (b) The aggregated active power, reactive power, spinning reserve, and regulating reserve submitted bids of AMGs for the day-ahead market considering the uncoordinated biddings of AMGs.

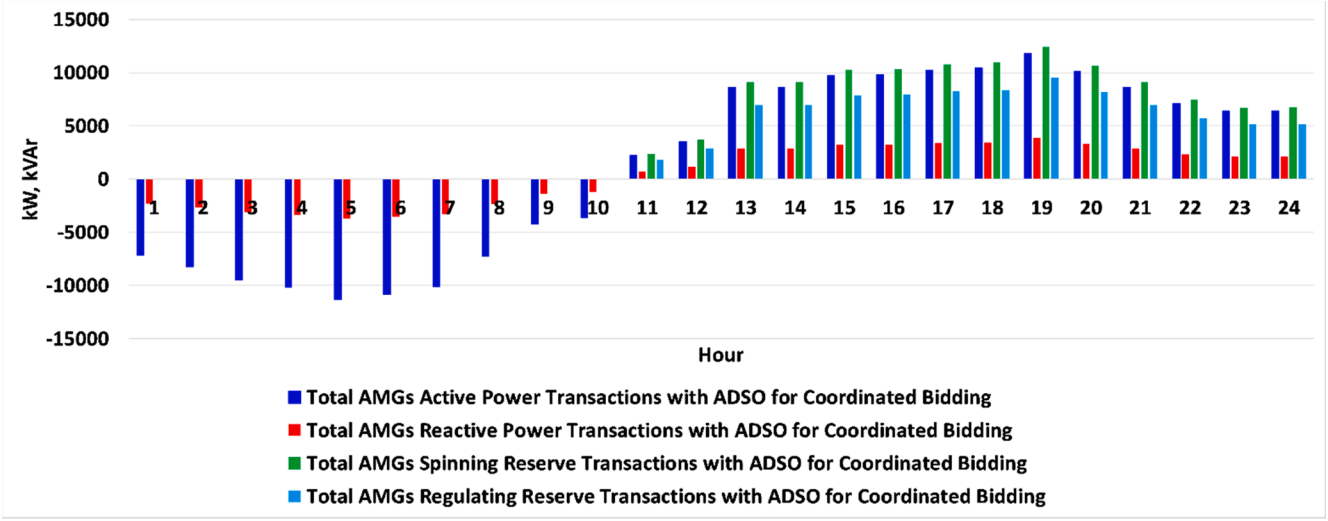

(a)

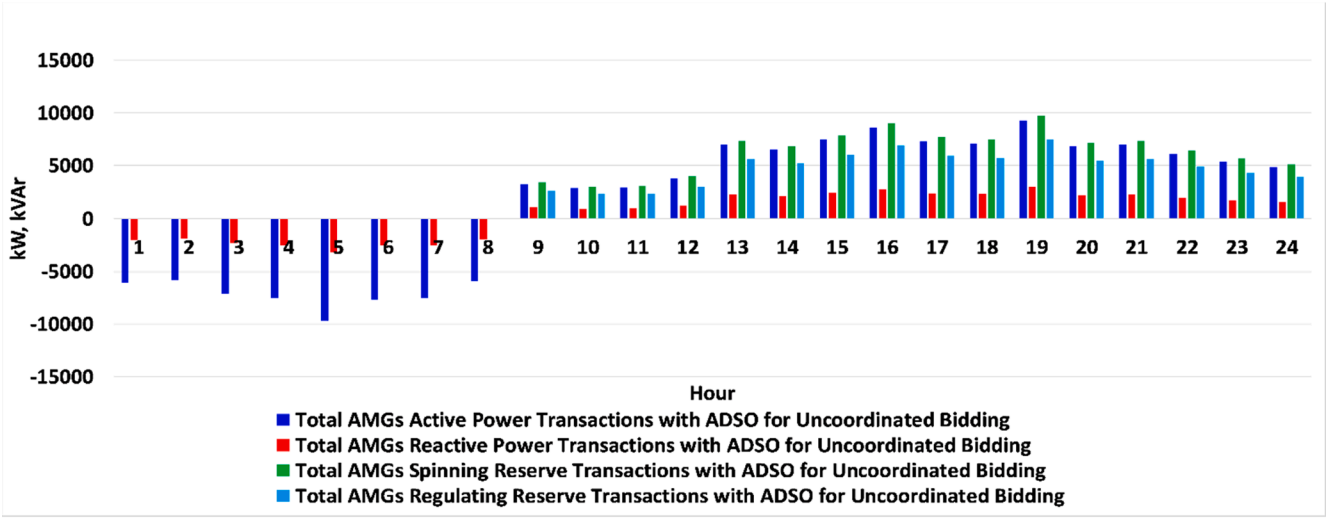

(b)

Fig. 15. (a) The aggregated active power, reactive power, spinning reserve, and regulating reserve transactions of AMGs with the ADSO for the day-ahead market considering the coordinated biddings of AMGs. (b) The aggregated active power, reactive power, spinning reserve, and regulating reserve transactions of AMGs with the ADSO for the day-ahead market considering the uncoordinated biddings of AMGs.

the proposed process was about 7681 seconds. It was assumed that each AMG was modeled as one distributed generation unit at its point of common coupling, which the facility's maximum active power capacity is presented in Table 2. The number of scenario generation, reduction, and characteristics of AMGs is also presented in Table 2. Table 3 presents the characteristics of MESSs. It was assumed that the available number of MESSs was equaled to the number of zones that the optimization process sectionalized the distribution system in external shock conditions.

Fig. 5 and Fig. 6 show the day-ahead forecasted load for one of the reduced scenarios and electricity generation of photovoltaic arrays for one of the reduced scenarios, respectively. Fig. 7 presents the electricity generation of wind turbine arrays for one of the reduced scenarios, respectively. Fig. 8 presents the day-ahead forecasted price of the active power and ancillary services for one of the reduced scenarios.

Fig. 9 (a) and Fig. 9 (b) present the dispatched values of active and reactive power of parking lots for the day-ahead market, respectively. As shown in Fig. 9 (a), the aggregated values of dispatched active and reactive powers of parking lots were 190932.21 kWh and 62721.23 kVArh, respectively. The average values of active power and reactive power were about 7955.509 kWh and 2613.38 kVArh, respectively. Figs. 9 (c) and (d) show the dispatched values of spinning reserve and regulating reserve of parking lots for the day-ahead market, respectively. As shown in Fig. 9 (c), the average value of dispatched spinning and regulating reserve of parking lots were about 8373.76 kW and 6330.15 kW, respectively.

Fig. 10 depicts the dispatched values of the active power of smart homes and energy transactions of ESSs. As shown in Fig. 10, the average and aggregate values of active power transactions of smart homes were about 433.39 kWh and 10401.59 kWh, respectively. Further, the average value of active power transactions of ESSs was about 208.87 kWh.

Fig. 11 (a) and Fig. 11 (b) depict the dispatched values of active power and reactive power of distributed generation facilities for the day-ahead market, respectively. As shown in Fig. 11 (a), the aggregated value of dispatched active and reactive power of distributed generations were 33452.22 kWh and 10989.05, respectively. The average values of active and reactive power of distributed generations were about 107.21 kWh and 35.22 kVArh, respectively.

Figs. 11 (c) and (d) present the dispatched values of spinning reserve

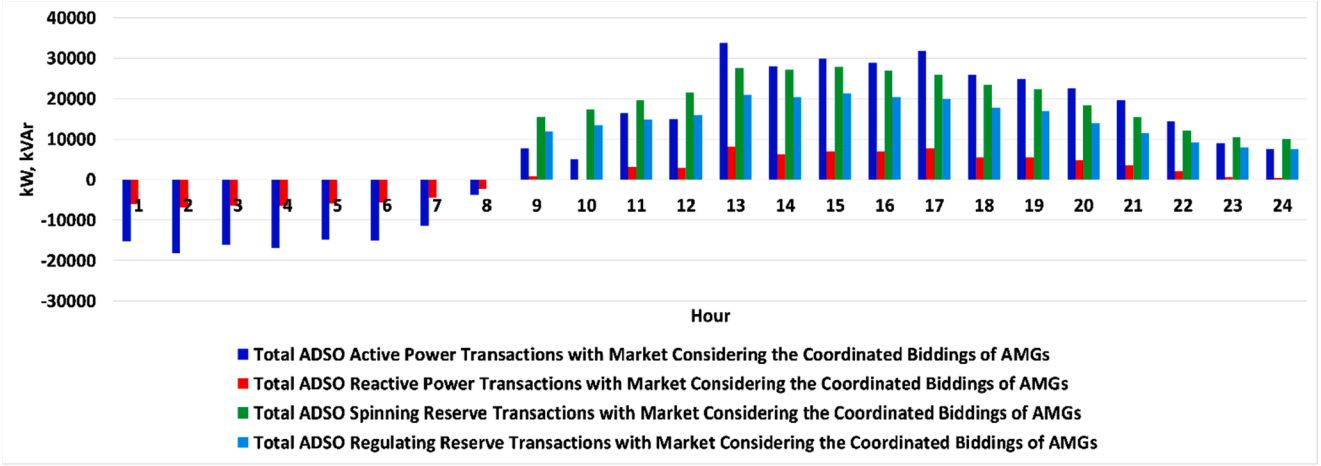

(a)

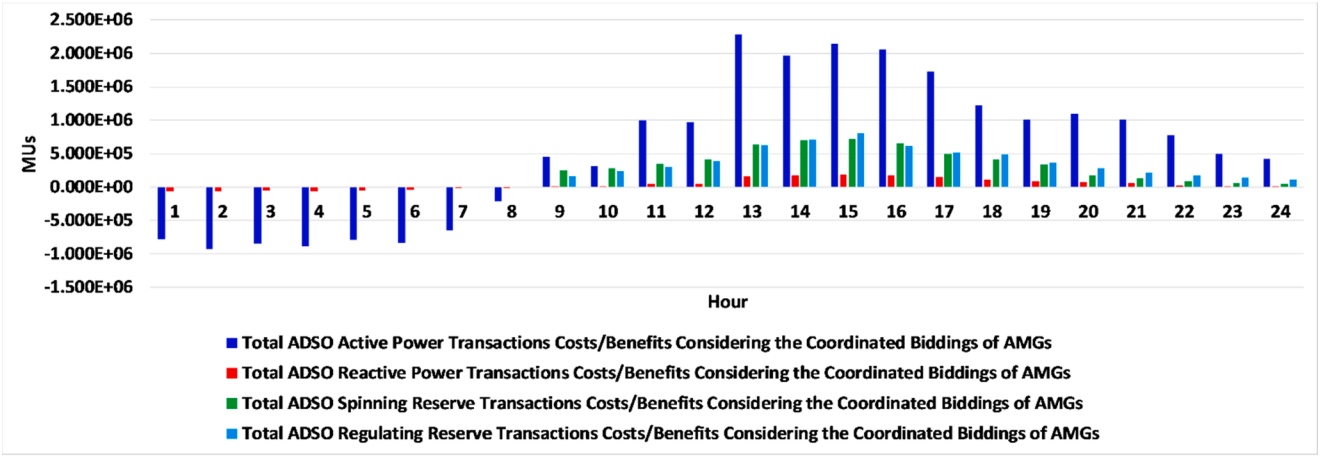

(b)

Fig. 16. (a) The active power, reactive power, spinning reserve, and regulating reserve transactions of the ADSO with the wholesale market for the day-ahead market considering the coordinated biddings of AMGs. (b) The cost/benefit of active power, reactive power, spinning reserve, and regulating reserve transactions of the ADSO with the wholesale market for the day-ahead market considering the coordinated biddings of AMGs.

and regulating reserve of distributed generation facilities for the day-ahead market, respectively. The average values of spinning reserve and regulating reserve of distributed generations were about 112.85 kW and 85.21 kW, respectively.

Fig. 12 depicts the electricity generation of CHPs for the day-ahead market. The aggregated active power generation of CHPs was about 126.64 MWh.

The scenario generation of AMGs' biddings is performed using the proposed objective functions for different values of bidding prices. Figs. 13 (a), (b), (c), and (d) show the coordinated and uncoordinated AMGs' submitted bids of active power, reactive power, spinning reserve, and regulating reserve respectively for one of the reduced scenarios and hour 11.

As shown in Figs. 13 (a), the AMGs submitted values for active power, reactive power, spinning reserve, and regulating reserve were highly increased when the AMGs coordinated their bidding strategy. For example, the AMG7 submitted 9116 MU and 11468 MU for uncoordinated and coordinated bidding conditions for a bidding power of 300 kW, respectively. Thus, the AMG7 increased the price of the submitted value for coordinated bidding conditions by about 25.81% concerning the uncoordinated bidding strategy to gain more profit.

Fig. 14 (a) shows the aggregated value of submitted bids of AMGs' active power, reactive power, spinning reserve, and regulating reserve to the ADSO database for the day-ahead market when the AMGs coordinated their biddings. Fig. 14 (b) shows the aggregated value of submitted bids of AMGs' active power, reactive power, spinning reserve, and regulating reserve to the ADSO database for the day-ahead market when the AMGs did not coordinate their biddings. As shown in Figs. 14 (a), (b), the aggregated value of submitted coordinated bids of AMGs' active power and reactive power were increased by about 20.21% and 20.27% respectively concerning the uncoordinated bidding conditions.

Fig. 15 (a) shows the aggregated active power, reactive power, spinning reserve, and regulating reserve transactions of AMGs with the ADSO for the day-ahead market when the AMGs coordinated their biddings. As shown in Fig. 15 (a), the AMGs imported active power and reactive power for 01:00 – 10:00 intervals. Further, the AMGs delivered active power, reactive power, spinning reserve, and regulating reserve for 11:00-24:00 intervals. The net active and reactive power transactions of AMGs with the ADSO were about 31204.78 kWh and 10250.77 kVArh, respectively. Fig. 15 (b) presents the aggregated active power, reactive power, spinning reserve, and regulating reserve transactions of AMGs with the ADSO for the day-ahead market when the AMGs did not coordinate their biddings. As shown in Fig. 13 (b), the AMGs imported active power and reactive power for 01:00 – 08:00 intervals. Further, the AMGs delivered active power, reactive power, spinning reserve, and regulating reserve for 09:00-24:00 intervals. The net active and reactive power transactions of AMGs with the ADSO were about 38959.09 kWh and 12798.06 kVArh, respectively.

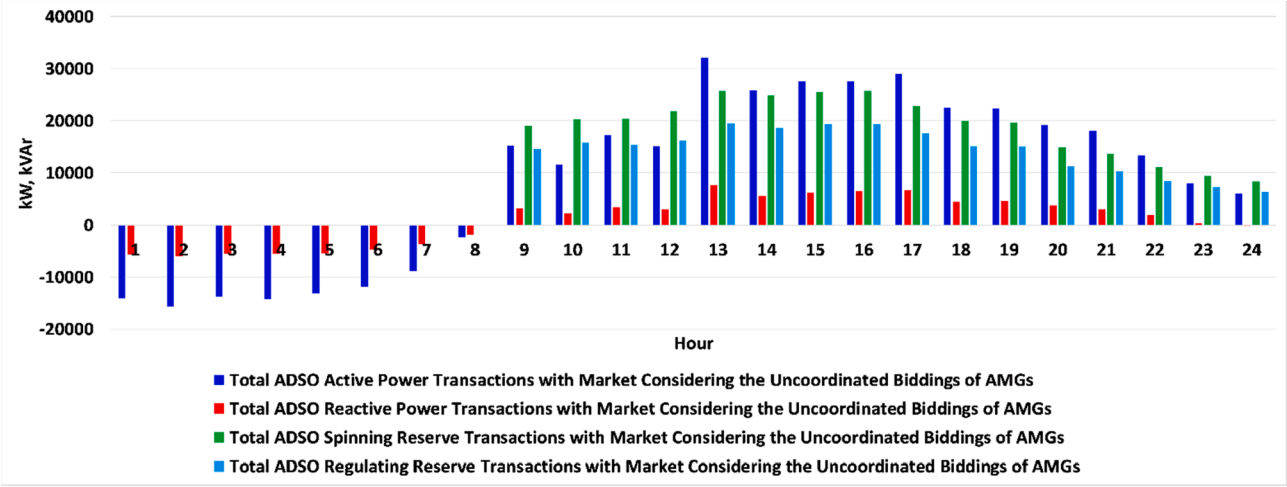

(a)

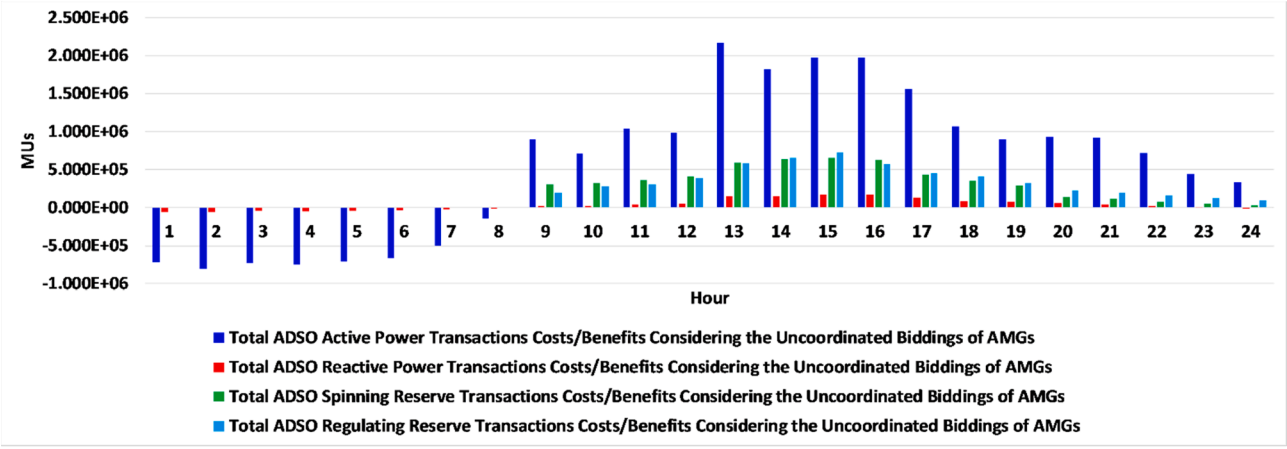

(b)

Fig. 17. (a) The active power, reactive power, spinning reserve, and regulating reserve transactions of the ADSO with the wholesale market for the day-ahead market considering the coordinated biddings of AMGs. (b) The cost/benefit of active power, reactive power, spinning reserve, and regulating reserve transactions of the ADSO with the wholesale market for the day-ahead market considering the coordinated biddings of AMGs.

Fig. 16 (a) presents the aggregated active power, reactive power, spinning reserve, and regulating reserve transactions of ADSO with the wholesale market considering the coordinated biddings of AMGs. The net active and reactive power transactions of ADSO with the wholesale market were about 209297.20 kWh and 21111.86 kVArh, respectively.

Fig. 16 (b) shows the aggregated cost/benefit of active power, reactive power, spinning reserve, and regulating reserve transactions of ADSO with the wholesale market considering the coordinated biddings of AMGs. The aggregated cost of active and reactive power transactions of ADSO with the wholesale market was about 13.94 MMUs. Further, the aggregated cost of spinning reserve and regulating reserve transactions of ADSO with the wholesale market was about 11.81 MMUs, respectively. MU stands for the monetary unit.

Fig. 17 (a) depicts the aggregated active power, reactive power, spinning reserve, and regulating reserve transactions of ADSO with the wholesale market considering the uncoordinated biddings of AMGs. The net active and reactive power transactions of ADSO with the wholesale market were about 217051.51 kWh and 23659.15 kVArh, respectively. Fig. 17 (b) presents the aggregated cost/benefit of active power, reactive power, spinning reserve, and regulating reserve transactions of ADSO with the wholesale market considering the uncoordinated biddings of AMGs. The aggregated cost of active and reactive power transactions of ADSO with the wholesale market was about 14.34 MMUs. Further, the aggregated cost of spinning reserve and regulating reserve transactions of ADSO with the wholesale market was about 11.11 MMUs, respectively. It can be concluded that the coordinated bidding of AMGs increased the aggregated costs of ADSO by about 1.18% for normal operating conditions.

Fig. 18 (a) depicts the number of zones for the 92 worst-case probable external shocks for the day-ahead optimization process (60 minutes intervals). The first level of the first stage optimization process determined the optimal topology of the system by sectionalizing of distribution system into multiple zones to mitigate the impact of external shocks.

Fig. 18 (b) presents the optimal allocating of MESSs for the 92 worst-case probable external shocks for the day-ahead optimization process (60 minutes intervals) considering the coordinated bidding of AMGs. The optimization process estimates the number of MESSs to recover the critical loads for the most credible external shocks.

Table 4 and Table 5 depict the optimal allocating of dispatched MESSs for the 80-92 worst-case probable external shocks considering the coordinated bidding of AMGs for the day-ahead scheduling process. As shown in Table 4 and Table 5, each MESS was allocated in the system buses in a preventive way to recover the maximum value of critical loads.

Fig. 19 (a) shows the SHI values for the day-ahead optimization horizon and 92 worst-case contingencies concerning the case without the MESSs allocations and system switching. As shown in Fig. 19 (a), the

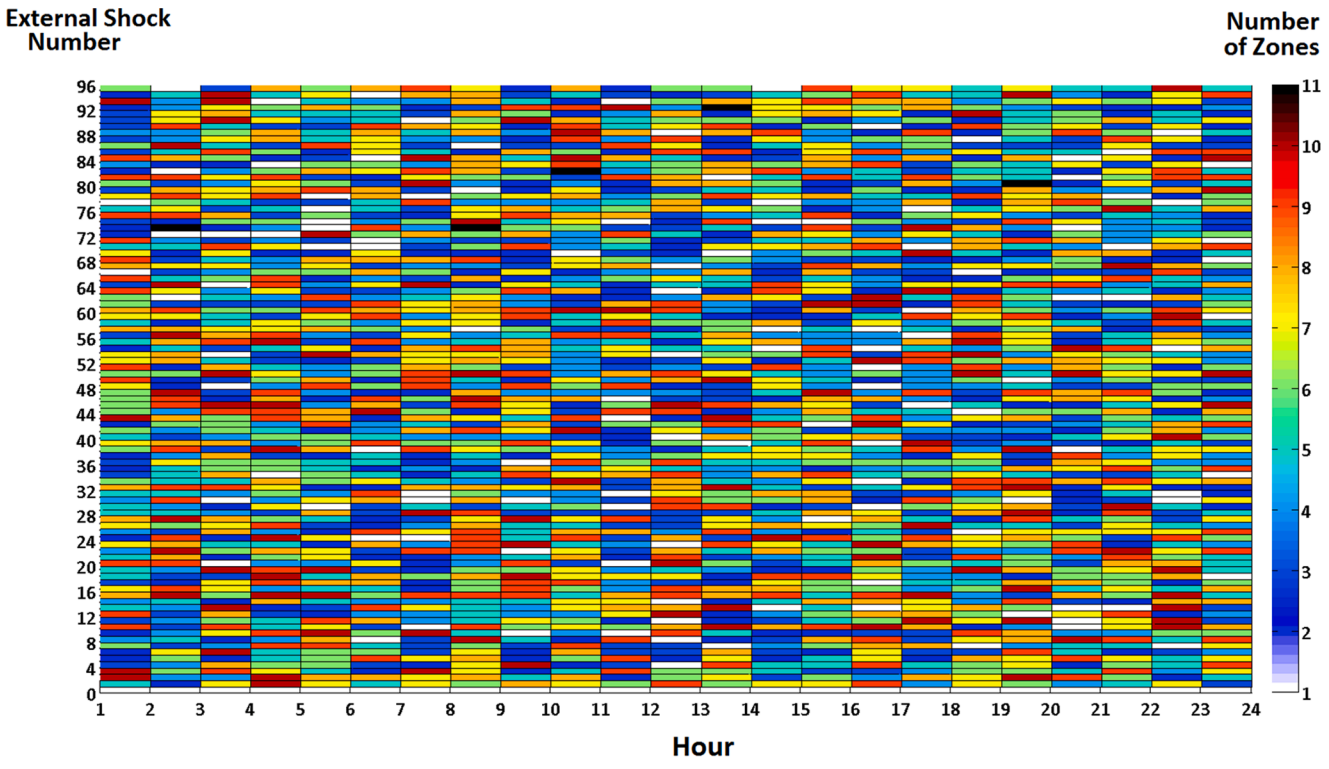

(a)

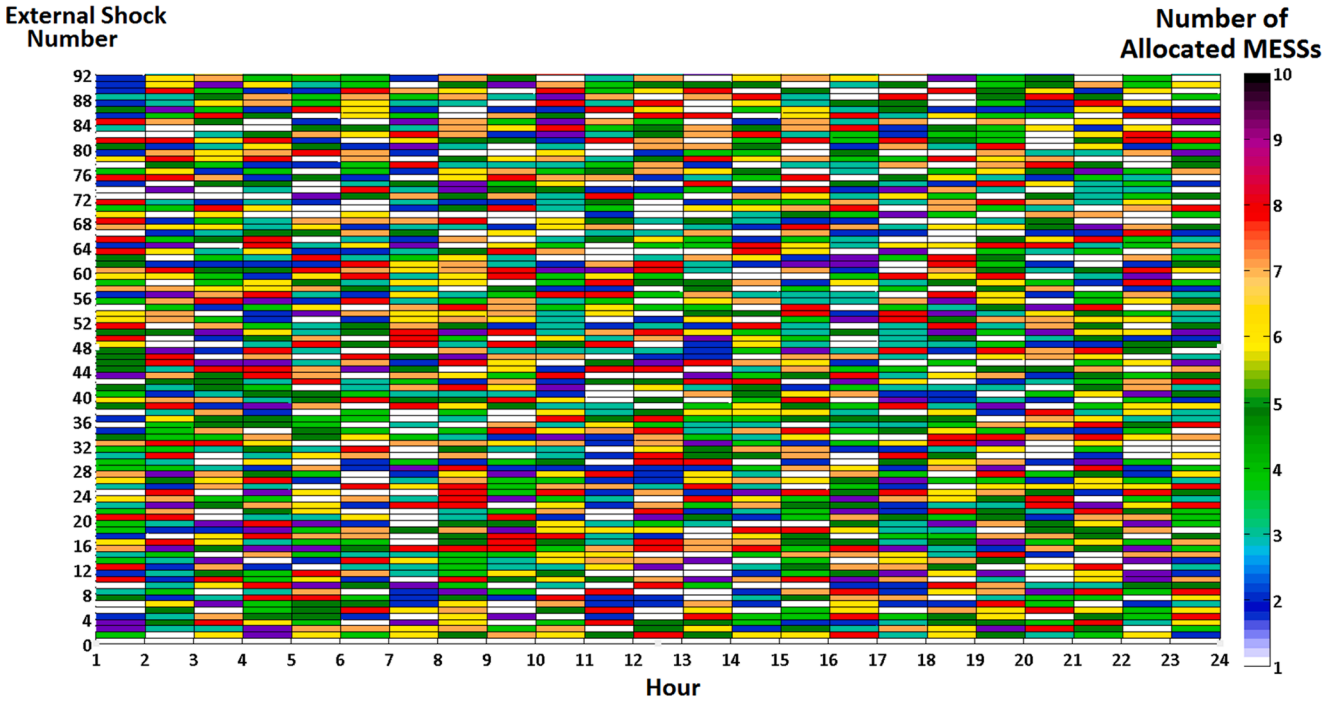

(b)

Fig. 18. (a). The number of zones for the 92 worst-case probable external shocks for the day-ahead optimization process (60 minutes intervals). (b) The optimal allocating of MESSs for the 92 worst-case probable external shocks for the day-ahead optimization process (60 minutes intervals).

average value of SHI took on a value of 0.659122. However, the SHI tended to be one for all of the considered 92-worst case external shocks. The maximum value of SHI was about 0.999617 for the 71st external shock and hour 18:00.

Further, Fig. 19 (b) presents the CGI values for the day-ahead optimization horizon and 92 worst-case contingencies concerning the case without the MESSs allocations and system switching. As shown in Fig. 19 (b), the average value of CGI took on a value of 0.5802. The maximum

Table 4
The optimal allocating of dispatched MESS1- MESS5 for the 80-92 worst-case probable external shocks.

MESS 1	Hour																							
External Shock	1	2	3	4	5	6	7	8	9	10	11	12	13	14	15	16	17	18	19	20	21	22	23	24
80	2	14	6	7	13	10	3	12	17	3	2	1	6	12	6	19	7	7	5	8	13	2	2	12
81	13	9	6	3	16	8	4	4	17	3	8	6	-	14	16	15	19	17	18	-	5	3	18	15
82	19	-	7	8	17	5	7	2	3	4	17	4	19	6	11	10	13	5	15	14	11	16	11	6
83	18	13	3	-	2	13	7	11	2	10	12	14	7	18	9	16	15	18	13	2	11	20	-	10
84	6	16	3	6	2	-	12	5	12	13	11	2	18	12	11	8	1	15	7	-	10	13	9	17
85	12	7	10	15	13	17	18	11	10	1	20	7	4	11	11	15	6	19	5	16	-	9	11	14
86	10	2	6	7	12	2	19	-	18	5	11	13	18	4	15	9	6	9	8	17	17	5	16	4
87	14	1	9	18	13	7	8	15	4	17	18	4	3	13	16	5	10	-	9	11	11	20	17	18
88	14	8	9	18	10	4	2	1	7	20	18	-	9	1	12	10	6	4	19	3	8	-	8	20
89	19	15	13	5	17	4	7	8	5	17	9	14	17	13	14	-	18	6	5	7	3	13	5	5
90	3	13	2	1	6	19	-	9	18	5	15	8	2	5	12	1	15	14	15	12	11	11	18	6
91	17	13	10	8	3	12	2	16	15	18	9	7	15	2	6	6	4	8	18	10	13	2	12	7
92	2	2	12	12	19	12	6	9	11	3	12	19	11	8	7	13	11	7	9	8	2	15	18	-
MESS 2	Hour																							
External Shock	1	2	3	4	5	6	7	8	9	10	11	12	13	14	15	16	17	18	19	20	21	22	23	24
80	32	32	32	22	23	32	26	30	-	23	-	28	30	27	-	23	26	27	21	-	26	31	25	30
81	29	28	26	32	22	-	23	29	32	22	24	31	-	22	31	21	24	31	24	-	30	25	31	27
82	-	-	22	28	25	29	33	28	23	25	26	22	28	30	30	23	31	31	25	-	31	23	31	22
83	33	-	-	-	23	30	25	24	30	30	25	31	32	28	29	21	31	33	32	26	32	26	-	26
84	23	31	24	-	25	-	33	30	29	27	30	24	-	23	28	26	28	-	27	-	31	-	32	32
85	23	27	24	30	-	27	24	-	32	23	-	23	23	-	23	22	31	26	32	32	-	26	30	29
86	31	23	23	30	28	23	29	-	25	23	24	25	-	26	22	21	27	22	27	25	28	24	28	30
87	26	22	32	29	22	27	29	32	-	33	25	27	-	23	25	22	26	-	32	23	31	30	-	25
88	29	24	23	22	25	25	28	23	26	22	29	-	31	25	30	-	25	-	22	29	29	-	31	24
89	32	26	25	25	23	27	23	28	-	26	28	23	26	-	33	-	-	28	33	26	32	21	-	26
90	30	27	28	29	24	24	-	23	27	24	25	25	32	33	-	27	28	-	31	22	22	24	22	27
91	29	23	27	28	27	24	25	25	32	-	24	28	-	22	28	28	-	21	28	22	-	25	-	26
92	-	25	24	24	23	32	-	29	26	22	22	24	28	27	23	31	33	31	24	31	-	-	24	-
MESS 3	Hour																							
External Shock	1	2	3	4	5	6	7	8	9	10	11	12	13	14	15	16	17	18	19	20	21	22	23	24
80	38	-	39	38	37	-	38	39	-	36	-	37	35	35	-	-	36	39	39	-	35	-	38	38
81	39	37	38	36	-	-	35	37	35	-	36	38	-	35	35	37	35	37	37	-	37	39	36	38
82	-	-	38	36	37	35	35	36	-	39	38	36	36	38	37	38	-	39	36	-	36	35	38	-
83	39	-	-	-	35	37	38	38	38	37	36	36	38	35	38	37	-	35	39	36	-	36	-	-
84	37	38	37	-	-	-	38	37	37	36	38	35	-	-	36	37	39	-	35	-	38	-	37	37
85	-	36	35	36	-	36	38	-	35	38	-	37	38	-	38	37	38	37	39	38	-	38	35	38
86	38	36	36	-	38	36	-	-	-	-	36	35	-	35	38	36	36	-	-	-	35	-	-	37
87	-	37	35	39	38	38	38	38	-	38	38	38	-	38	36	37	35	-	35	-	36	36	-	37
88	37	35	37	39	36	35	38	38	37	37	38	-	36	35	35	-	39	-	36	35	37	-	36	38
89	-	35	35	-	-	37	37	35	-	37	38	37	37	-	39	-	-	39	37	38	-	37	-	37
90	-	39	38	39	36	37	-	37	38	39	35	35	36	38	-	38	35	-	35	36	39	37	37	38
91	-	35	36	38	37	35	-	37	38	-	38	35	-	39	38	35	-	38	35	35	-	37	-	37
92	-	37	39	38	37	37	-	-	38	39	39	39	39	39	36	36	37	37	36	-	-	-	38	-
MESS 4	Hour																							
External Shock	1	2	3	4	5	6	7	8	9	10	11	12	13	14	15	16	17	18	19	20	21	22	23	24
80	49	-	-	41	47	-	43	-	-	-	-	50	48	49	-	-	42	-	47	-	46	-	51	-
81	46	44	48	51	-	-	48	43	47	-	43	49	-	47	48	46	47	48	49	-	46	45	47	-
82	-	-	-	41	47	43	48	41	-	46	-	49	50	45	-	46	-	43	42	-	42	47	46	-
83	-	-	-	-	48	44	-	42	48	50	47	43	43	42	43	43	-	46	51	41	-	42	-	-
84	46	49	43	-	-	-	48	44	50	41	49	47	-	-	44	-	41	-	44	-	43	-	42	41
85	-	43	47	41	-	48	49	-	46	51	-	46	45	-	46	49	-	47	45	44	-	45	45	45
86	42	47	49	-	49	41	-	-	-	-	40	46	-	44	43	-	44	-	-	-	43	-	-	45
87	-	-	44	47	45	49	-	-	-	50	-	48	-	50	-	44	42	-	45	-	42	48	-	-
88	-	-	50	41	43	49	40	43	-	49	45	-	44	45	-	-	42	-	47	51	49	-	49	47
89	-	46	43	-	-	42	44	42	-	46	40	47	44	-	44	-	-	41	49	50	-	50	-	43
90	-	41	46	48	-	42	-	49	48	44	47	50	47	46	-	-	48	-	49	41	43	50	44	48
91	-	50	43	50	47	40	-	51	47	-	-	51	-	41	46	41	-	47	50	51	-	41	-	-
92	-	-	49	45	51	43	-	-	43	40	47	-	48	44	44	50	42	41	-	-	-	-	-	-
MESS 5	Hour																							
External Shock	1	2	3	4	5	6	7	8	9	10	11	12	13	14	15	16	17	18	19	20	21	22	23	24
80	60	-	-	59	52	-	61	-	-	-	-	59	59	58	-	-	58	-	57	-	57	-	-	-
81	56	59	61	57	-	-	53	59	52	-	55	54	-	-	60	-	53	60	-	-	54	54	55	-
82	-	-	-	53	59	58	53	58	-	54	-	55	60	61	-	-	-	-	-	-	56	52	-	-
83	-	-	-	-	53	59	-	60	59	52	-	55	57	60	57	54	-	59	-	53	-	56	-	-
84	55	57	59	-	-	-	57	58	-	59	61	-	-	-	58	-	59	-	55	-	53	-	57	54
85	-	-	53	54	-	60	-	-	58	55	-	58	53	-	57	56	-	60	-	-	-	61	53	-
86	52	52	-	-	60	60	-	-	-	-	57	56	-	-	57	-	59	-	-	-	57	-	-	-
87	-	-	57	52	-	55	-	-	-	53	-	55	-	55	-	59	57	-	-	-	53	53	-	-
88	-	-	57	55	-	61	-	57	-	57	53	-	59	59	-	-	57	-	53	57	57	-	-	56
89	-	57	-	-	-	58	55	59	-	54	-	59	57	-	54	-	-	54	57	60	-	55	-	58
90	-	57	60	59	-	-	-	59	52	55	-	56	58	60	-	-	56	-	-	57	55	-	58	54
91	-	56	60	-	-	-	-	58	58	-	-	54	-	55	60	55	-	54	-	60	-	-	-	-
92	-	-	56	54	58	56	-	-	56	60	56	-	55	57	54	59	60	59	-	-	-	-	-	-

value of CGI was about 0.938574 for the 19th external shock and hour 11:00.

The real-time load forecasting process was performed for the 15 minutes intervals. Fig. 20 shows the real-time electrical load forecasting mismatches for different forecasting intervals. For example, Delta (3, 1) presents the mismatches between the base load forecasting and the updated values that were calculated for the second 15-minute interval.

Fig. 21 (a) presents the available ramp of parking lots, DGs, AMGs, ESSs, and the provided ramp of ADS considering the coordinated bidding of AMGs. As shown in Fig. 21 (a), the parking lots, DGs, AMGs, and ESSs did not provide the ramp of ADS for many 15 minutes intervals and the distribution system provided the ramp from the wholesale market. Fig. 21 (b) presents the available ramp of parking lots, DGs, AMGs, ESSs, and the provided ramp of ADS considering the uncoordinated bidding of AMGs. By comparing Fig. 21 (a) and Fig. 21 (b), it can be concluded that the coordinated biddings of AMGs decreased the available ramp service by about 11.42%, based on the fact that the AMGs endeavored to maximize their profits through coordinated

Table 5
The optimal allocating of dispatched MESS6- MESS9 for the 80-92 worst-case probable external shocks.

MESS 6	Hour																						
External Shock	1	2	3	4	5	6	7	8	9	10	11	12	13	14	15	16	17	18	19	20	21	22	23	24
80	-	-	-	93	-	-	94	-	-	-	-	93	95	-	-	-	92	-	94	-	92	-	-	-
81	94	94	96	92	-	-	94	-	-	-	93	91	-	-	93	-	96	-	-	-	-	95	96	-
82	-	-	-	-	95	94	93	93	-	93	-	-	95	93	-	-	-	-	-	-	93	92	-	-
83	-	-	-	-	-	-	-	92	96	96	-	-	95	-	92	94	-	-	-	95	-	92	-	-
84	94	94	-	-	-	-	94	92	-	92	92	-	-	-	94	-	96	-	92	-	91	-	96	-
85	-	-	95	-	-	92	-	-	95	-	-	94	95	-	93	94	-	91	-	-	-	93	94	-
86	-	93	-	-	92	92	-	-	-	-	96	94	-	-	92	-	-	-	-	-	93	-	-	-
87	-	-	92	93	-	93	-	-	-	94	-	92	-	92	-	-	-	-	-	-	94	94	-	-
88	-	-	-	95	-	92	-	94	-	93	96	-	91	96	-	-	92	-	-	93	-	-	-	93
89	-	93	-	-	-	95	96	94	-	91	-	91	92	-	-	-	-	93	-	92	-	92	-	95
90	-	92	92	94	-	-	-	-	92	93	-	-	-	-	-	-	-	-	-	-	93	-	94	92
91	-	93	96	-	-	-	-	94	-	-	-	94	-	94	92	91	-	91	-	-	-	-	-	-
92	-	-	96	-	94	-	-	-	94	94	95	-	91	91	92	-	95	-	-	-	-	-	-	-
MESS 7	Hour																							
External Shock	1	2	3	4	5	6	7	8	9	10	11	12	13	14	15	16	17	18	19	20	21	22	23	24
80	-	-	-	-	-	-	87	-	-	-	-	88	87	-	-	-	88	-	86	-	-	-	-	-
81	88	88	-	86	-	-	-	-	-	-	89	88	-	-	86	-	87	-	-	-	-	89	87	-
82	-	-	-	-	87	-	89	87	-	89	-	-	87	90	-	-	-	-	-	-	-	89	-	-
83	-	-	-	-	-	-	-	86	-	88	-	-	89	-	86	90	-	-	-	-	-	-	-	-
84	88	89	-	-	-	-	90	86	-	87	90	-	-	-	87	-	88	-	89	-	-	-	89	-
85	-	-	88	-	-	-	-	-	87	-	-	87	87	-	-	87	-	-	-	-	-	87	89	-
86	-	89	-	-	89	-	-	-	-	-	89	-	-	-	-	-	-	-	-	-	-	-	-	-
87	-	-	-	86	-	-	-	-	-	87	-	90	-	-	-	-	-	-	-	-	86	-	-	-
88	-	-	-	88	-	89	-	88	-	90	90	-	90	88	-	-	88	-	-	89	-	-	-	-
89	-	90	-	-	-	89	88	-	-	88	-	-	87	-	-	-	-	88	-	-	-	-	-	-
90	-	-	88	-	-	-	-	-	87	87	-	-	-	-	-	-	-	-	-	-	86	-	-	87
91	-	-	88	-	-	-	-	87	-	-	-	87	-	-	88	-	-	88	-	-	-	-	-	-
92	-	-	-	-	88	-	-	-	86	86	87	-	86	-	-	-	87	-	-	-	-	-	-	-
MESS 8																								
External Shock	1	2	3	4	5	6	7	8	9	10	11	12	13	14	15	16	17	18	19	20	21	22	23	24
80	-	-	-	-	-	-	79	-	-	-	-	-	-	-	-	-	-	-	85	-	-	-	-	-
81	74	73	-	76	-	-	-	-	-	-	82	-	-	-	75	-	80	-	-	-	-	72	74	-
82	-	-	-	-	-	-	77	-	-	79	-	-	-	78	-	-	-	-	-	-	-	79	-	-
83	-	-	-	-	-	-	-	-	-	77	-	-	-	-	-	72	-	-	-	-	-	-	-	-
84	78	-	-	-	-	-	77	-	-	75	-	-	-	-	-	-	-	-	-	-	-	-	77	-
85	-	-	76	-	-	-	-	-	-	-	-	74	82	-	-	80	-	-	-	-	-	84	84	-
86	-	73	-	-	74	-	-	-	-	-	72	-	-	-	-	-	-	-	-	-	-	-	-	-
87	-	-	-	-	-	-	-	-	-	80	-	80	-	-	-	-	-	-	-	-	76	-	-	-
88	-	-	-	-	-	-	-	-	-	73	-	-	-	82	-	-	85	-	-	84	-	-	-	-
89	-	80	-	-	-	75	-	-	-	72	-	-	77	-	-	-	-	84	-	-	-	-	-	-
90	-	-	74	-	-	-	-	-	75	-	-	-	-	-	-	-	-	-	-	-	-	-	-	-
91	-	-	-	-	-	-	-	-	-	-	-	-	-	-	-	-	-	78	-	-	-	-	-	-
92	-	-	-	-	-	-	-	-	75	78	83	-	83	-	-	-	-	-	-	-	-	-	-	-
MESS 9	Hour																							
External Shock	1	2	3	4	5	6	7	8	9	10	11	12	13	14	15	16	17	18	19	20	21	22	23	24
80	-	-	-	-	-	-	112	-	-	-	-	-	-	-	-	-	-	-	-	-	-	-	-	-
81	-	-	-	-	-	-	-	-	-	-	-	-	-	-	-	-	-	-	-	-	-	-	-	-
82	-	-	-	-	-	-	-	-	-	107	-	-	-	-	-	-	-	-	-	-	-	-	-	-
83	-	-	-	-	-	-	-	-	-	-	-	-	-	-	-	-	-	-	-	-	-	-	-	-
84	-	-	-	-	-	-	105	-	-	106	-	-	-	-	-	-	-	-	-	-	-	-	101	-
85	-	-	-	-	-	-	-	-	-	-	-	-	-	-	-	-	-	-	-	-	-	-	-	-
86	-	101	-	-	-	-	-	-	-	-	-	-	-	-	-	-	-	-	-	-	-	-	-	-
87	-	-	-	-	-	-	-	-	-	-	-	-	-	-	-	-	-	-	-	-	-	-	-	-
88	-	-	-	-	-	-	-	-	-	102	-	-	-	-	-	-	-	-	-	-	-	-	-	-
89	-	-	-	-	-	-	-	-	-	-	-	-	-	-	-	-	-	-	-	-	-	-	-	-
90	-	-	102	-	-	-	-	-	100	-	-	-	-	-	-	-	-	-	-	-	-	-	-	-
91	-	-	-	-	-	-	-	-	-	-	-	-	-	-	-	-	-	100	-	-	-	-	-	-
92	-	-	-	-	-	-	-	-	-	-	103	-	104	-	-	-	-	-	-	-	-	-	-	-

bidding of ramp services. ~

Fig. 22 (a) depicts the aggregated operating and interruption costs of ADSO for the 92 worst-case external shocks concerning the coordinated bidding of AMGs without implementing the proposed algorithm for the real-time optimization process (15 minutes intervals). The worst-case external shock was the 80th contingency that occurred at 19:30-19:45 intervals. As shown in Fig. 22 (a), the aggregated operating and interruption cost of ADSO was about 29372045.42 MUs for the worst-case external shock condition when the ADSO did not consider the proposed algorithm. The average value of the aggregated operating and interruption cost of ADSO was about 2459258.76 MUs for the 92 worst-case external shocks.

The aggregated operating and interruption cost of ADSO was about 11161377.26 MUs for the worst-case external shock condition considering the coordinated bidding of AMGs and implementation of the proposed algorithm. The average value of the aggregated operating and interruption costs of ADSO was about 979655.82 MUs for the mentioned conditions. Thus, the proposed algorithm reduced the average value of aggregated operating and interruption costs of ADSO by about 60.16% considering the coordinated bidding of AMGs for the worst-case external shock.

The simulation result for the most credible external shock is presented. The system topology for the most credible external shock (80th external shock) is shown in Fig. 23. The external shock was compromised in two contingencies. The first contingency occurred in the 13-152 line and the second contingency occurred in the 160-67 line. The optimal allocations of MESSs in nodes are displayed in red color. The preventive optimization process allocated the MESSs in the following bus: 5, 21, 39, 47, 57, 94, 86, and 85. The proposed method sectionalized the distribution system into eleven zones and the MESSs were optimally allocated in zones to supply the critical loads.Fig 24.

Fig. 22 (a) and Fig. 22 (b) present the committed loads of active and passive smart homes for the most credible external shock concerning the case without the MESSs allocations and system switching. As shown in

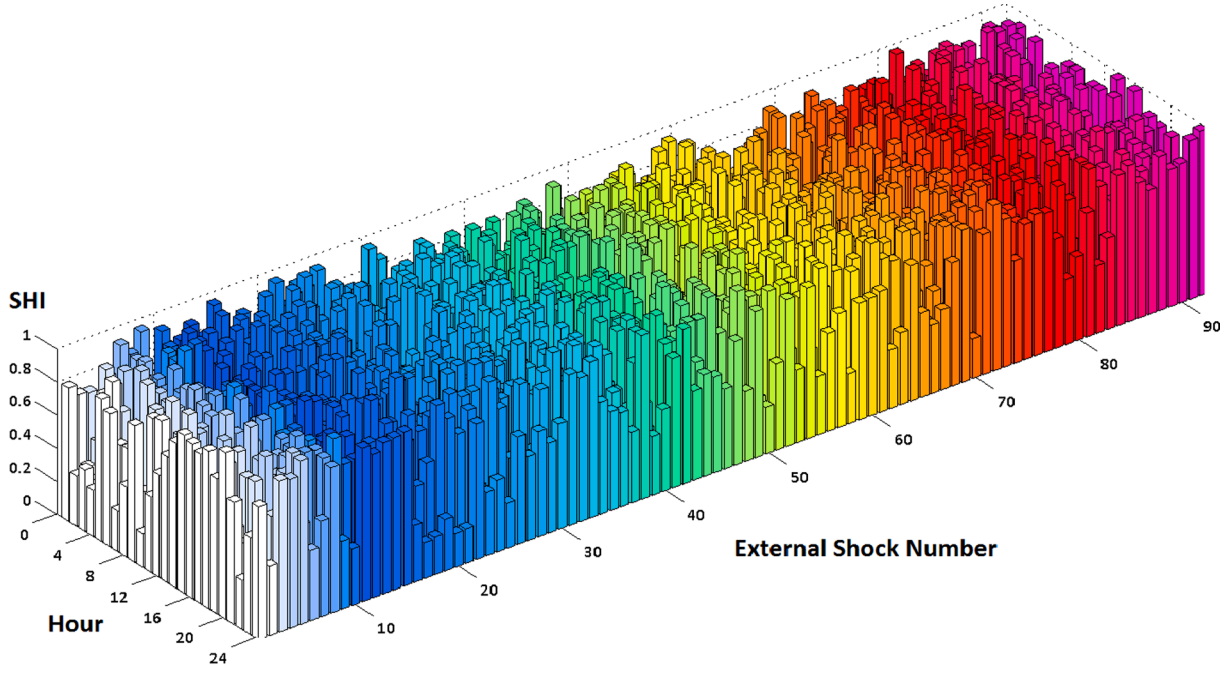

(a)

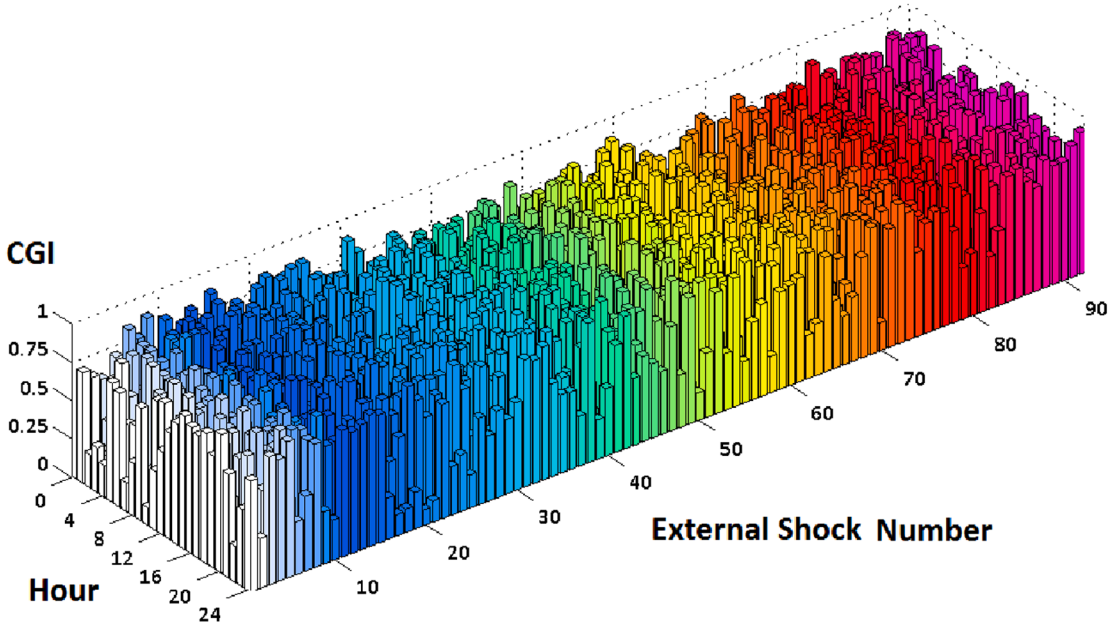

(b)

Fig. 19. (a) The SHI values for the day-ahead optimization horizon and 92 worst-case contingencies concerning the case without the MESSs allocations and system switching, (b) The CGI values for the day-ahead optimization horizon and 92 worst-case contingencies concerning the case without the MESSs allocations and system switching.

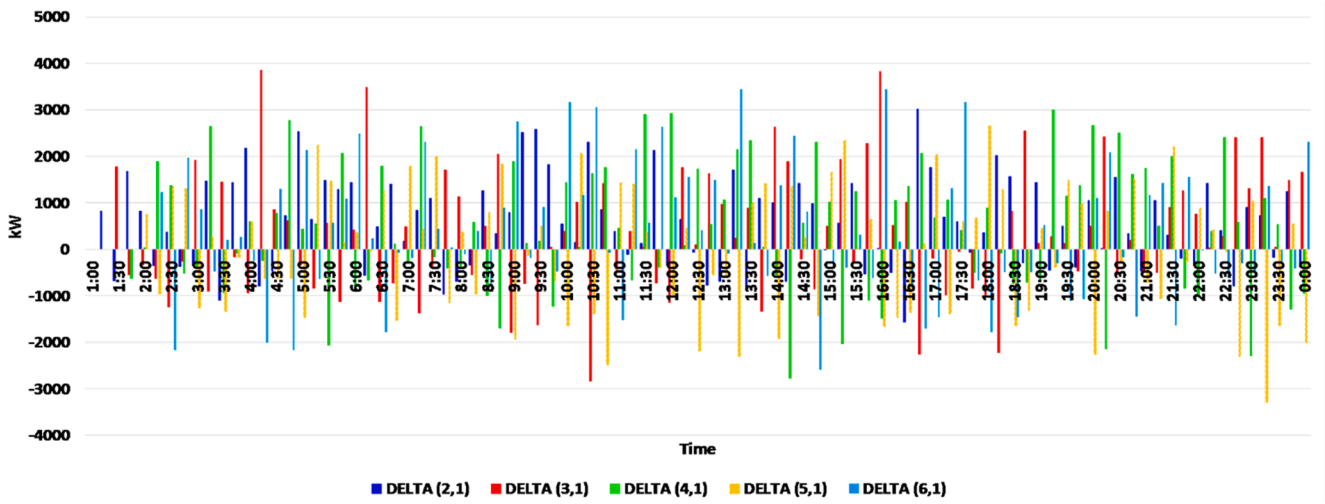

Fig. 20. The real-time electrical load forecasting mismatches for different forecasting intervals.

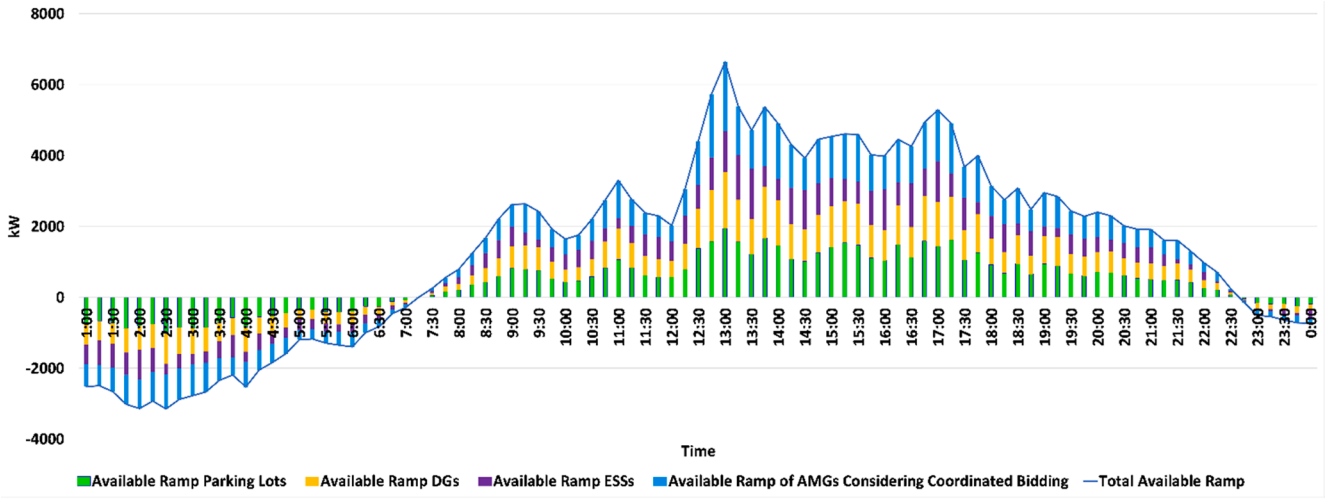

(a)

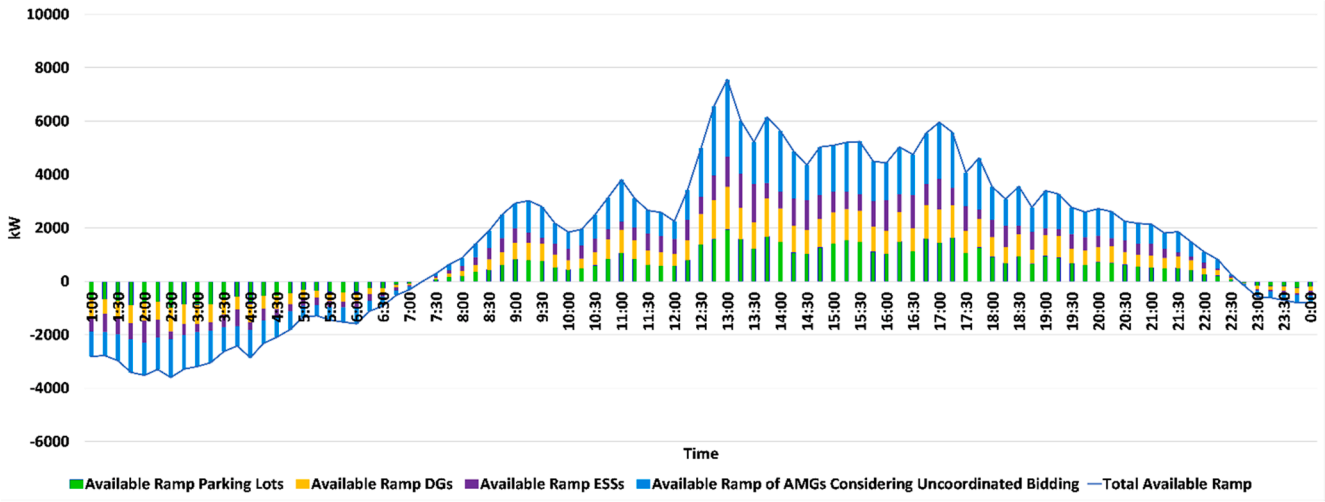

(b)

Fig. 21. (a) The available ramp of parking lots, DGs, AMGs, ESSs, and the provided ramp of ADS considering the coordinated bidding of AMGs. (b) The available ramp of parking lots, DGs, AMGs, ESSs, and the provided ramp of ADS considering the uncoordinated bidding of AMGs.

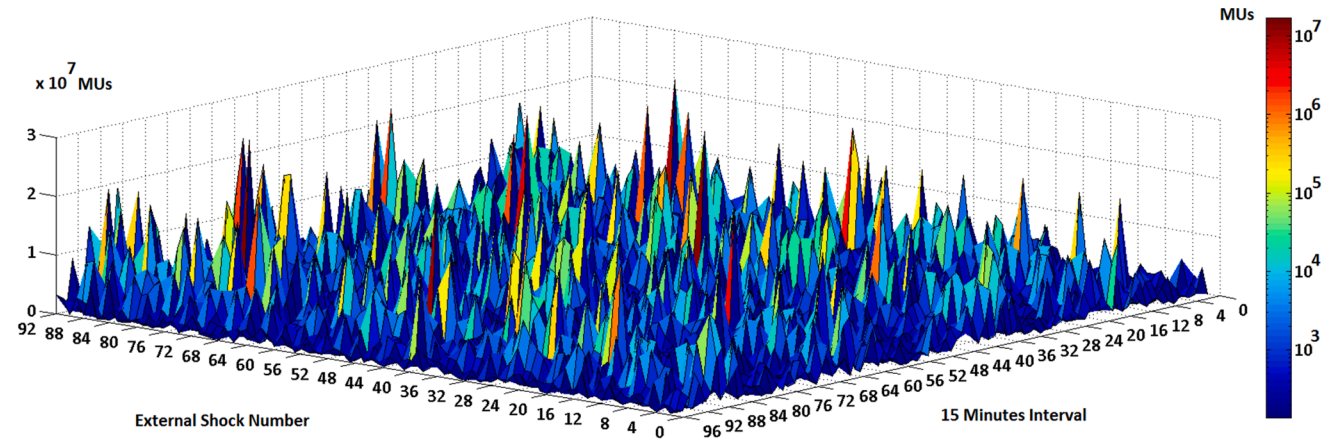

(a)

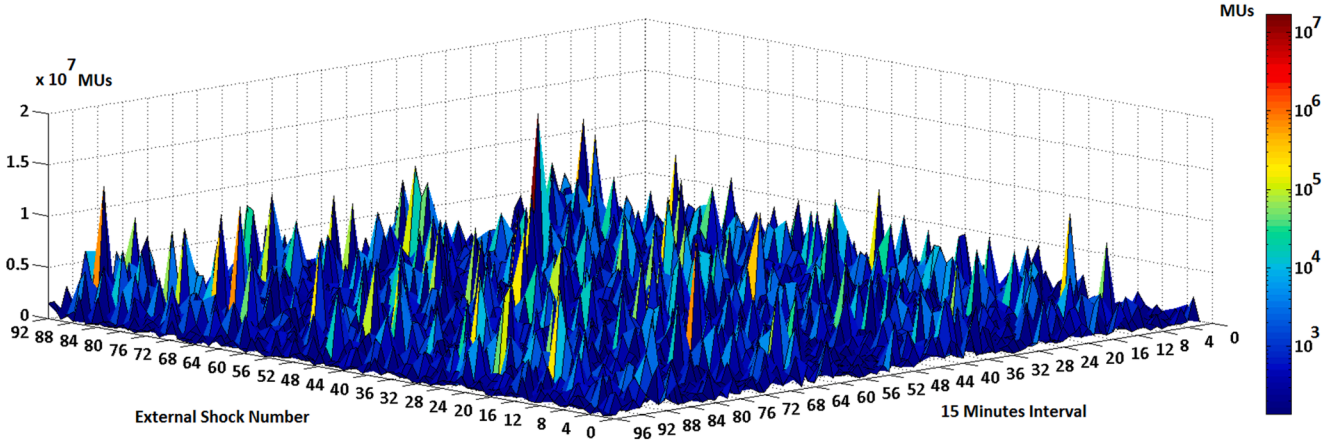

(b)

Fig. 22. (a) The aggregated operating and interruption costs of ADSO for the 92 worst-case external shocks concerning the coordinated bidding of AMGs and without implementing the proposed algorithm for the real-time optimization process, (b) the aggregated operating and interruption costs of ADSO for the 92 worst-case external shocks concerning the coordinated bidding of AMGs and implementing the proposed algorithm for the real-time optimization process.

Figs. 22, the aggregated electrical loads of active and passive smart homes were 2032.36 kWh and 445.83 kWh, respectively. However, the aggregated committed electrical loads of active and passive smart homes were 1243.08 kWh and 310.34 kWh, respectively. Concerning the case without the MESSs allocations and system switching, the optimization process committed the electrical loads of active and passive smart homes by about 61.16% and 69.60% concerning their initial values, respectively. The self-healing index took on a value of 0.6672 for the most credible external shock concerning the case without the MESSs allocations and system switching. However, the self-healing index took on a value of one for the most credible external shock concerning the MESSs allocations and switching case based on the fact that the algorithm successfully recovered all of the critical and non-critical loads using MESSs and switching of system switches.

Two sensitivity analyses were carried out to assess the impacts of the number of available MESSs and the capacity of MESSs on the optimization process outputs.

Table 6 presents the sensitivity analysis results for assessing the impacts of the number of available MESSs on the self-healing index, coordination gain index, and aggregated operating and interruption costs of ADSO for the worst-case external shock condition considering the coordinated bidding of AMGs and implementing the proposed algorithm and the case without implementing the proposed algorithm.

As shown in Table 6, the self-healing index decreased when the number of available MESSs was decreased. Further, the coordination gain index and aggregated operating and interruption costs of ADSO for the worst-case external shock condition were highly increased when the number of available MESSs was decreased. The average value of the self-healing index was reduced by about 26.8% when the number of available MESSs was decreased to six number concerning the A_1 case.

Table 7 presents the impacts of the capacity of MESSs on the aggregated operating and interruption costs of ADSO for the worst-case

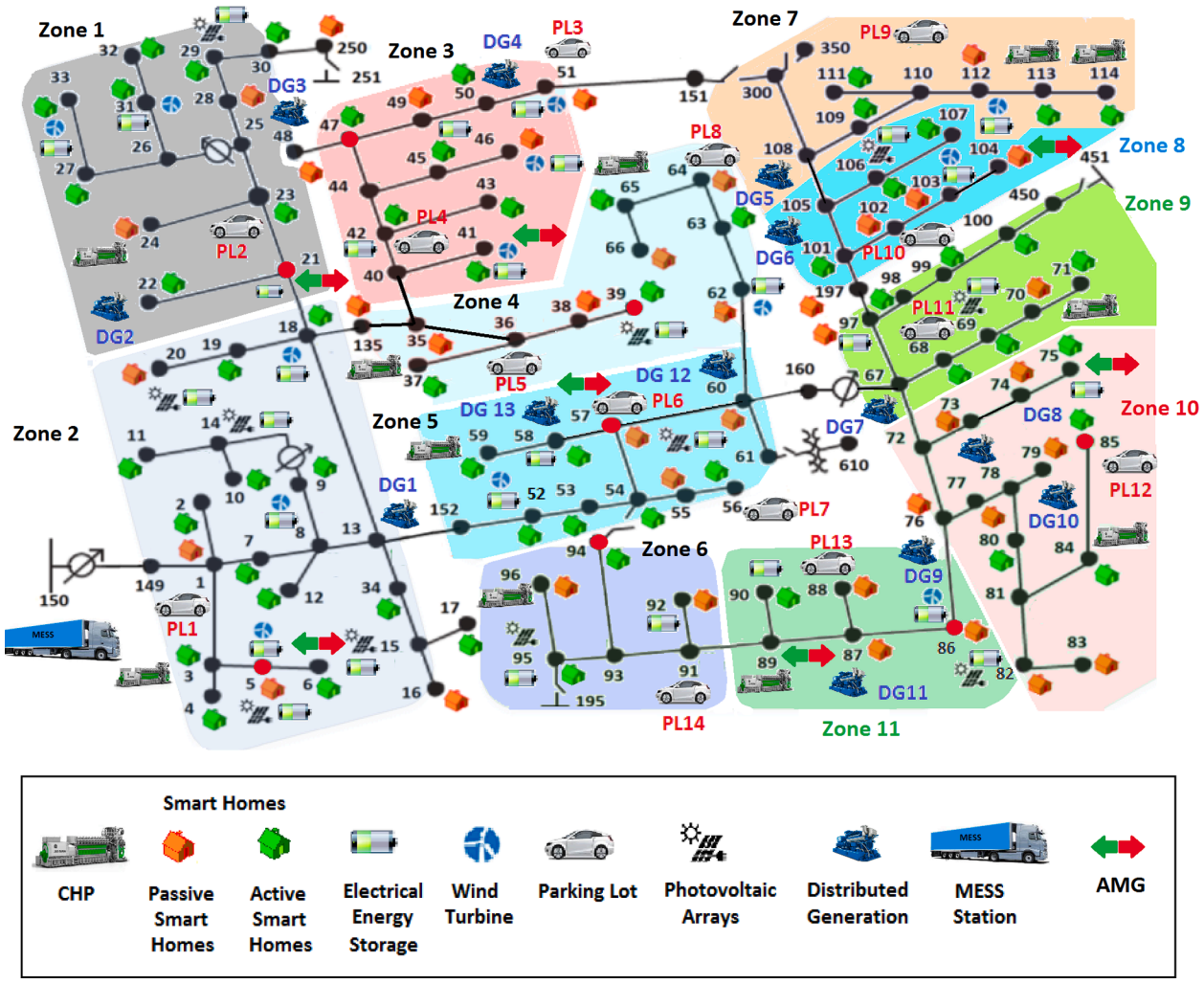

Fig. 23. The sectionalizing process of the distribution system for the worst-case external shocks.

external shock condition considering the coordinated bidding of AMGs and implementation of the proposed algorithm, self-healing index, and coordination gain index.

As shown in Table 7, the self-healing index was decreased when the capacity of MESSs was decreased. Further, the coordination gain index and aggregated operating and interruption costs of ADSO for the worst-case external shock condition were increased when the capacity of MESSs was decreased. The aggregated operating and interruption cost of ADSO was reduced by about 1.413% when the capacity of MESSs was increased to 500 kWh concerning the base case.

In conclusion, the proposed optimization process modeled the active power, reactive power, spinning reserve, and regulating reserve transaction in the day-ahead market by the ADS, AMGs, and wholesale market. Further, the active power, reactive power, and ramp service transactions in the real-time market were modeled. The optimal location of MESSs and switching of ADS switches were considered to reduce the impacts of external shocks. Further, the load commitment process of smart homes was modeled. The impacts of the coordinated bidding of AMGs on the system's resiliency were modeled. Finally, the proposed method successfully reduced the impacts of the most credible external shocks and increased the resiliency of the distribution system concerning the optimal allocation of MESSs and switching of the system.

5. Conclusion

This paper introduced a multi-stage framework for the optimal resilient allocation of mobile energy storage facilities concerning the coordinated bidding of microgrids in day-ahead and real-time markets. The framework compromises day-ahead and real-time stages. The first level of the day-ahead optimization process determined the locations of MESSs in a preventive and utilized the sectionalizing process of the system to reduce the impacts of probable shocks. Then, the bidding process of microgrids was simulated in the second level of the first stage. Finally, the optimization procedure of system energy resources was carried out in the third level of the first stage. The real-time problem was categorized into the normal state and shock conditions problems. If there was not any shock condition, the real-time problem optimized the dispatch of energy resources of AMGs and ADSO, respectively. If there was an external shock condition, the optimal topology of the system was optimized in a corrective way in the first level. Then, the optimal scheduling of the AMGs and ADSO were determined in the second and third levels, respectively. The self-healing and coordination gain indices were proposed to assess the resiliency of the system and the profit of microgrids through coordinated bidding, respectively. The self-healing index took on a value of 0.6672 for the most credible external shock

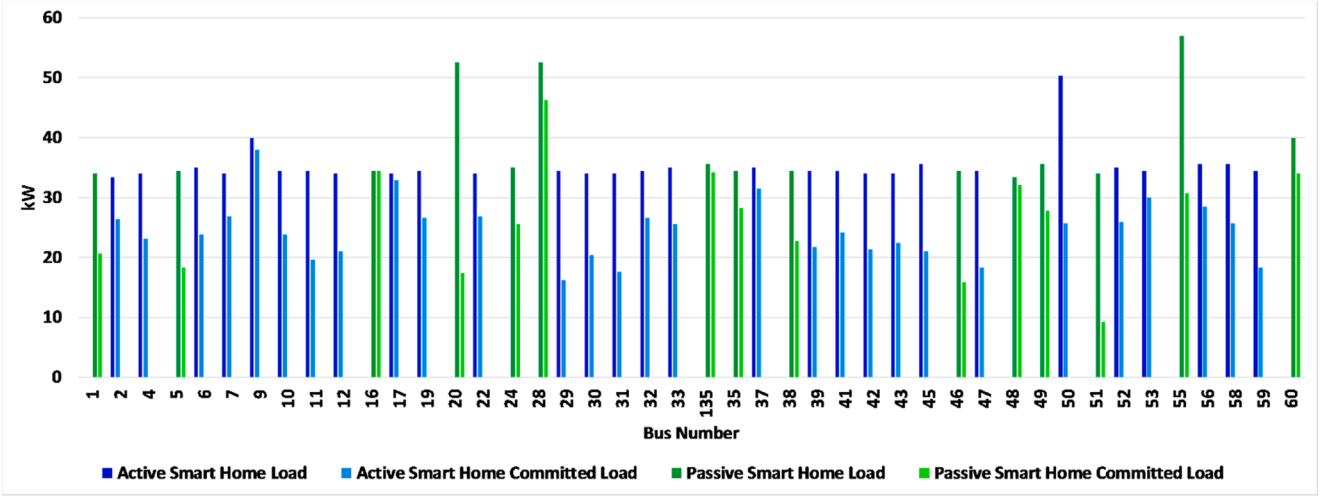

(a)

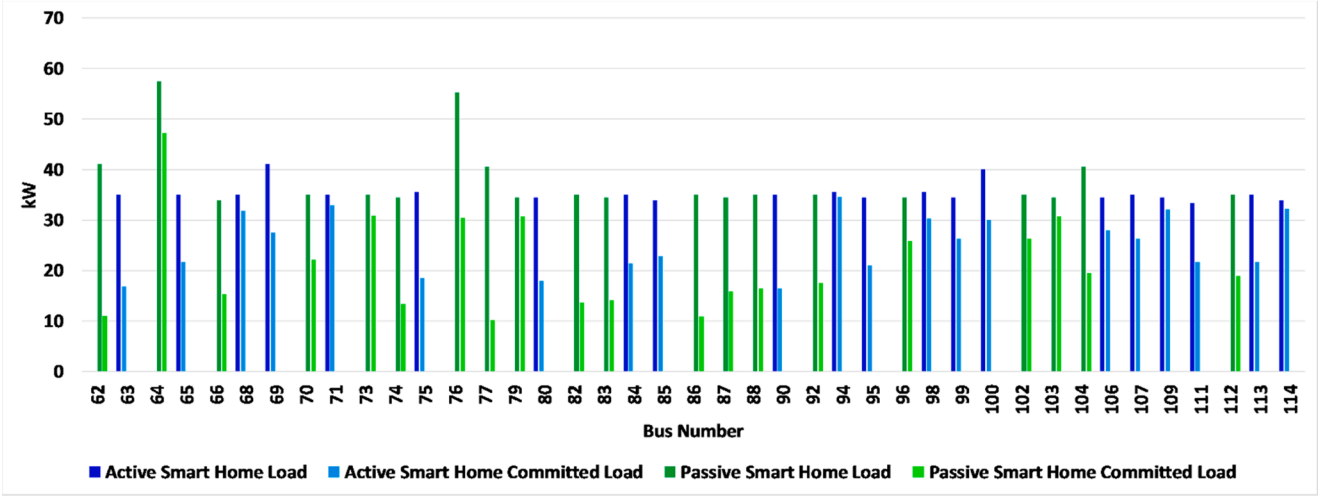

(b)

Fig. 24. (a) The direct load control of 1st - 60th smart homes for the most credible external shock. (b) The direct load control of 62nd - 114th smart homes for the most credible external shock.

Table 6
The sensitivity analysis results for assessing the impacts of the number of available MESSs on the optimization process outputs.

Number of available MESS	B_1	B_2	B_3	B_4	B_5
0	0.999617	0.659122	0.938574	0.5802	29372045.42
A_1	1	1	0.216912	0.1236	11161377.26
10	0.999991	0.823146	0.321891	0.1492	13986212.93
8	0.999848	0.769314	0.449817	0.1987	16874521.71
6	0.999732	0.731925	0.593665	0.2971	21559817.21
A_1	Number of available MESS was equaled maximum number of zones that determined by the optimization process considering the coordinated bidding of AMGs and implementing the proposed algorithm				
B_1	Maximum Value of Self-healing index				
B_2	Average Value of Self-healing index				
B_3	Maximum Value of Coordination gain index				
B_4	Average Value of Coordination gain index				
B_5	Aggregated operating and interruption costs of ADSO for the worst-case external shock condition (MUs)				

Table 7
The sensitivity analysis results for assessing the impacts of the number of available MESSs on the optimization process outputs.

Capacity of MESS (kWh)	C_1	C_2	C_3	C_4	C_5
0	0.999617	0.659122	0.938574	0.5802	29372045.42
300	1	1	0.216912	0.1236	11161377.26
200	0.999912	0.763621	0.286911	0.1295	14982328.39
100	0.999835	0.716932	0.392817	0.2193	16932847.35
400	1	1	0.206932	0.1199	11092539.64
500	1	1	0.186916	0.1039	11003645.31
C_1	Maximum Value of Self-healing index				
C_2	Average Value of Self-healing index				
C_3	Maximum Value of Coordination gain index				
C_4	Average Value of Coordination gain index				
C_5	Aggregated operating and interruption costs of ADSO for the worst-case external shock condition (MUs)				

concerning the case without the MESSs allocations and system switching. Finally, the proposed algorithm reduced the average value of aggregated operating and interruption costs of ADSO by about 60.16% considering the coordinated bidding of AMGs for the worst-case external shock. The authors are working on the simulation of other distributed energy resources for the proposed framework.

CRediT authorship contribution statement

Ainollah Rahimi Sadegh: Investigation, Data curation, Writing – original draft. **Mehrdad Setayesh Nazar:** Conceptualization, Methodology, Supervision. **Miadreza Shafie-khah:** Formal analysis, Validation. **João P.S. Catalão:** Visualization, Writing – review & editing.

Declaration of Competing Interest

The authors declare that they have no known competing financial interests or personal relationships that could have appeared to influence the work reported in this paper.

Data availability

The data that has been used is confidential.

Acknowledgment

J.P.S. Catalão acknowledges the support by FEDER funds through COMPETE 2020 and by Portuguese funds through FCT, under POCI-01-0145-FEDER-029803 (02/SAICT/2017).

References

[1] Aboutalebi M, Setayesh Nazar M, Shafie-khah M, Catalão JPS. Optimal scheduling of self-healing distribution systems considering distributed energy resource capacity withholding strategies. Int J Electr Power Energy Syst 2022;136:107662.
[2] Wang Y, Oulis Rousis A, Strbac G. Resilience-driven optimal sizing and pre-positioning of mobile energy storage systems in decentralized networked microgrids. Appl Energy 2022;305:117921.
[3] Saboori H, Jadid S. Mobile and self-powered battery energy storage system in distribution networks–Modeling, operation optimization, and comparison with stationary counterpart. J Energy Storage 2021;4:103068.
[4] Khardenavis A, Hewage K, Perera P, Mohammadpour Shotorbani A, Sadiq R. Mobile energy hub planning for complex urban networks: A robust optimization approach. Energy 2021;235:121424.
[5] Wang H, Yan Z, Shahidehpour M, Zhou Q, Xu X. Optimal energy storage allocation for mitigating the unbalance in active distribution network via uncertainty quantification. IEEE Trans Sustainable Energy 2021;12:303–13.
[6] Erenŏglu A, Erdinç O. Post-Event restoration strategy for coupled distribution-transportation system utilizing spatiotemporal flexibility of mobile emergency generator and mobile energy storage system. Electric Power Syst Res 2021;199:107432.
[7] Jiang X, Chen J, Wu Q, Zhang W, Zhang Y, Liu J. Two-step optimal allocation of stationary and mobile energy storage systems in resilient distribution networks. J Modern Power Syst Clean Energy 2021;9:788–99.
[8] Mehrjerdi H, Mahdavi S, Hemmati R. Resilience maximization through mobile battery storage and diesel DG in integrated electrical and heating networks. Energy 2021;237:121195.
[9] S. Amin Sedgh, M. Doostizadeh, F. Aminifar, M. Shahidehpour, " Resilient-enhancing critical load restoration using mobile power sources with incomplete information", *Sustainable Energy, Grids and Networks*, 2121, 26, 100418.
[10] Hosseinnia H, Modarresi J, Nazarpour D. Optimal eco-emission scheduling of distribution network operator and distributed generator owner under employing demand response program. Energy 2020;191:116553.
[11] Fotouhi Ghazvini MA, Soares J, Abrishambaf O, Castro R, Vale Z. Demand response implementation in smart households". Energy Build 2017;143:129–48.
[12] Rahimi K, Davoudi M. Electric vehicles for improving resilience of distribution systems. Sustainable Cities and Soc 2018;36:246–56.
[13] Guo Z, Li G, Zhou M, Feng W. Resilient configuration approach of integrated community energy system considering integrated demand response under uncertainty. IEEE Access 2019;7:87513–33.
[14] Eseye A, Lehtonen M, Tukia T, Uimonen S, Millar R. Optimal energy trading for renewable energy integrated building microgrids containing electric vehicles and energy storage batteries. IEEE Access 2019;7:106092–101.
[15] F. Hafiz, B. Chen, C. Chen, A.R. de Queiroz, I. Husain, "Utilising demand response for distribution service restoration to achieve grid resiliency against natural disasters", 2019, *IET Gener. Transm. Distrib*., 13, pp. 2942-2950.
[16] Mehrjerdi H, Hemmati R. Coordination of vehicle-to-home and renewable capacity resources for energy management in resilience and self-healing building". Renew Energy 2020;146:568–79.
[17] Hussain A, Bui VH, Kim HM. A resilient and privacy-preserving energy management strategy for networked microgrids". IEEE Trans on Smart Grid 2016;9:2127–39.
[18] Hussain A, Bui VH, Kim HM. Microgrids as a resilience resource and strategies used by microgrids for enhancing resilience. Appl Energy 2019;240:56–72.
[19] T. Khalili, M. Tarafdar Hagh, S. Gassem Zadeh, S. Maleki,"Optimal reliable and resilient construction of dynamic self-adequate multi-microgrids under large-scale events", *IET Gener. Transm. Distrib*., 2019, 10, pp. 1750 . 1760.
[20] Wang Z, Wang J. Self-healing resilient distribution systems based on sectionalization into microgrids. IEEE Trans on Power Sys 2015;30:3139–49.
[21] Chanda S, Srivastava AK. Defining and enabling resiliency of electric distribution systems with multiple microgrids". IEEE Trans on Smart Grid 2016;7:2859–68.
[22] Zhu J, Yuan Y, Wang W. An exact microgrid formation model for load restoration in resilient distribution system". Int J Electr Power Energy Syst 2020;116:105568.
[23] Farzin H, Fotuhi-Firuzabad M, Moeini-Aghtaie M. Enhancing power system resilience through hierarchical outage management in multi-microgrids. IEEE Trans on Smart Grid 2016;7:2869–79.
[24] Zakernezhad H, Setayesh Nazar M, Shafie-khah MR, Catalão JPS. Optimal resilient operation of multi-carrier energy systems in electricity markets considering distributed energy resource aggregators. Appl Energy 2021;299:117271.
[25] Heitsch H, Römisch W. Scenario reduction algorithms in stochastic programming". Comput Optimization and Applications 2003;24:187–206.
[26] Lobato FS, Steffen Jr V. Multi-objective optimization problems concepts and self-adaptive parameters with mathematical and engineering applications. Springer Press; 2017.
[27] Kavousi-Fard A, Zare A, Khodaei A. Effective Dynamic Scheduling of Reconfigurable Microgrids. IEEE Trans on Power Syst 2018;33(5):5519–30.